cmgh
CELLULAR AND MOLECULAR GASTROENTEROLOGY AND HEPATOLOGY

ORIGINAL RESEARCH

Ethanol and its Nonoxidative Metabolites Promote Acute Liver Injury by Inducing ER Stress, Adipocyte Death, and Lipolysis

Seol Hee Park,[1,*] Wonhyo Seo,[1,2,*] Ming-Jiang Xu,[1] Bryan Mackowiak,[1] Yuhong Lin,[1] Yong He,[1] Yaojie Fu,[1] Seonghwan Hwang,[1] Seung-Jin Kim,[1] Yukun Guan,[1] Dechun Feng,[1] Liqing Yu,[3] Richard Lehner,[4] Suthat Liangpunsakul,[5,6,7] and Bin Gao[1]

[1]*Laboratory of Liver Diseases, National Institute on Alcohol Abuse and Alcoholism, National Institutes of Health, Bethesda, Maryland;* [2]*Laboratory of Hepatotoxicity, College of Pharmacy, Ewha Womans University, Seoul, Republic of Korea;* [3]*Department of Medicine, University of Maryland School of Medicine, Baltimore, Maryland;* [4]*Departments of Cell Biology and Pediatrics, Group on Molecular & Cell Biology of Lipids, University of Alberta, Edmonton, Canada;* [5]*Division of Gastroenterology and Hepatology, Department of Medicine, Indiana University School of Medicine, Indianapolis, Indiana;* [6]*Department of Biochemistry and Molecular Biology, Indiana University School of Medicine, Indianapolis, Indiana; and* [7]*Roudebush Veterans Administration Medical Center, Indianapolis, Indiana*

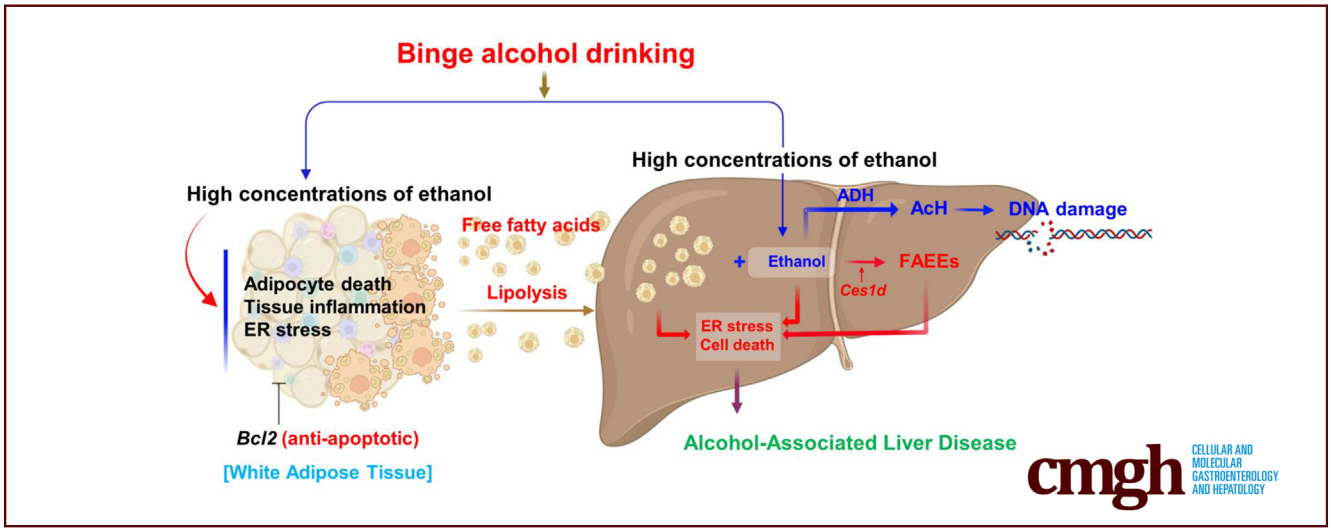

SUMMARY

Binge drinking induces acute liver injury and is an important risk factor for alcohol-associated liver disease. Binge alcohol and its nonoxidative metabolites promote acute liver injury by inducing endoplasmic reticulum stress, adipocyte death, and lipolysis.

BACKGROUND & AIMS: Binge drinking in patients with metabolic syndrome accelerates the development of alcohol-associated liver disease. However, the underlying mechanisms remain elusive. We investigated if oxidative and nonoxidative alcohol metabolism pathways, diet-induced obesity, and adipose tissues influenced the development of acute liver injury in a single ethanol binge model.

METHODS: A single ethanol binge was administered to chow-fed or high-fat diet (HFD)-fed wild-type and genetically modified mice.

RESULTS: Oral administration of a single dose of ethanol induced acute liver injury and hepatic endoplasmic reticulum (ER) stress in chow- or HFD-fed mice. Disruption of the *Adh1* gene increased blood ethanol concentration and exacerbated acute ethanol-induced ER stress and liver injury in both chow-fed and HFD-fed mice, while disruption of the *Aldh2* gene did not affect such hepatic injury despite high blood acetaldehyde levels. Mechanistic studies showed that alcohol, not acetaldehyde, promoted hepatic ER stress, fatty acid synthesis, and increased adipocyte death and lipolysis, contributing to acute liver injury. Increased serum fatty acid ethyl esters (FAEEs), which are formed by an enzyme-mediated esterification of ethanol with fatty acids, were detected in mice after ethanol gavage, with higher levels in *Adh1* knockout mice than in wild-type mice. Deletion of the *Ces1d* gene in mice markedly reduced the acute ethanol-induced increase of blood FAEE levels with a slight but significant reduction of serum aminotransferase levels.

CONCLUSIONS: Ethanol and its nonoxidative metabolites, FAEEs, not acetaldehyde, promoted acute alcohol-induced liver injury by inducing ER stress, adipocyte death, and lipolysis. *(Cell Mol Gastroenterol Hepatol 2023;15:281–306; https://doi.org/10.1016/j.jcmgh.2022.10.002)*

Keywords: Binge; ADH; ALDH; FAEE; Carboxylesterase 1d.

Alcohol-associated liver disease (ALD) is a major cause of chronic liver diseases.[1] It represents a spectrum of histopathologic changes from steatosis, steatohepatitis, cirrhosis, and hepatocellular carcinoma. The risk of ALD is associated with the quantity of alcohol consumed. Patients with alcohol-induced steatosis who continue to consume more than 400 g/wk alcohol significantly increase their risk for cirrhosis.[2] In another large study of more than 13,000 patients, the risk for ALD increased considerably with drinking more than 7–13 alcoholic beverages per week in women and 14 to 27 alcoholic beverages per week in men.[3] In addition to the quantity of alcohol consumed, the pattern of drinking also is associated with the development of ALD. Binge drinking, a heavy episodic alcohol intake, is defined as consuming 5 or more drinks on an occasion for men or 4 or more drinks on an occasion for women.[4] It is a drinking pattern associated with an increase in blood alcohol concentration above the legal limit within 2 hours.[4] Binge drinking is thought to be an important risk factor for ALD observed in millennials[5,6] and patients with metabolic syndrome.[7,8] However, the underlying mechanisms of binge drinking–associated ALD remain elusive.

Once ingested, alcohol is metabolized, primarily in the liver, by oxidative and nonoxidative pathways.[9] More than 90% of ingested alcohol is converted into acetaldehyde by oxidative enzymes, alcohol dehydrogenase (ADH), cytochrome P450 2E1 (CYP2E1), and catalase.[9] Many adverse effects of ethanol among chronic drinkers are mediated by its byproduct, acetaldehyde.[10] Acetaldehyde is metabolized further into acetate by mitochondrial aldehyde dehydrogenase 2 (ALDH2) in the liver. Interestingly, our recent studies suggest that liver ALDH2 is responsible for less than 50% of blood acetaldehyde clearance.[11] In addition, a nonoxidative pathway to metabolize alcohol is mediated by the generation of lipophilic fatty acid ethyl esters (FAEEs), a combination of alcohol with free fatty acids.[12] The generation of FAEEs is mediated by tissue-specific FAEE synthase enzymes, FAEE carboxylesterase (encoded by *Ces1d* in murine and *CES1* in human beings) in the liver, and *Cel* in the pancreas.[13–15] FAEEs accumulate in tissues after acute alcohol intoxication, causing organ inflammation and injury.[12] The implications of binge drinking on oxidative and nonoxidative pathways in association with liver injury remain obscure.

The pathogenesis of ALD is complex and interorgan crosstalk between the liver and other tissues contributes to the progression of ALD.[16] Interorgan crosstalk leads to inflammation, metabolic alternations, and cell death in ALD.[16] Adipose tissue is an important organ in regulating lipid homeostasis.[17] Chronic alcohol consumption markedly increases adipocyte death[18] and lipolytic activity in murine adipose tissue.[19,20] An increase in adipose tissue lipolysis causes the release of nonesterified free fatty acids, providing an extrahepatic source of free fatty acids for accumulation in hepatocytes, causing hepatic steatosis by the esterification process to triglycerides.[21] The role of adipose tissue in binge alcohol consumption and liver injury remains elusive.

The development of the chronic-plus-binge ethanol model has led to the discovery of multiple pathways in ALD pathogenesis.[22–26] However, the molecular mechanisms underlying binge ethanol–induced liver injury have not been investigated carefully. To address these mechanisms, we used a single ethanol binge model in several genetically modified mouse models to identify the pathways linking binge drinking, obesity, and acute liver injury. There is a challenge in developing a preclinical model for binge alcohol consumption in rodents.[27] The amount of alcohol consumed in human beings during a binge episode, which may lead to liver injury, is approximately 0.8–1 g/kg in a 70-kg subject.[4] In mice, ethanol metabolism and clearance are approximately 5.5-fold faster than that in human beings.[27] We therefore carefully selected the quantity of alcohol being administered in our mouse model at 5–7 g/kg. By using this model, here we investigated the role of a single ethanol binge and acute liver injury by focusing on the following objectives. First, we examined if oxidative and nonoxidative alcohol metabolism pathways influence the development of acute liver injury. Second, we explored the implications of a single ethanol binge and diet-induced obesity on acute liver injury. Third, we determined the role of the liver and adipose tissue crosstalk in the pathogenesis of liver injury after a single ethanol binge.

Results

A Single Ethanol Binge Induces Acute Liver Injury in Mice via the Induction of Endoplasmic Reticulum Stress

A single ethanol binge via oral gavage to C57BL/6N mice induced liver injury in a dose-dependent manner, from 5 to 7 g/kg of ethanol (Figure 1*A*). The highest peak of

***Authors share co-first authorship.**

Abbreviations used in this paper: **ADH, alcohol dehydrogenase; ALD, alcohol-associated liver disease; ALDH2, aldehyde dehydrogenase 2; ALT, alanine aminotransferase; AST, aspartate aminotransferase; cDNA, complementary DNA; CHOP, C/EBP Homologous Protein; CLS, crown-like structure; CYP2E1, cytochrome p450 2E1; eIF2α, –; ER, endoplasmic reticulum; FAEE, fatty acid ethyl ester; FFA, free fatty acid; GTT, glucose tolerance test; HFD, high-fat diet; HSL, hormone-sensitive lipase; IRE1α, Inositol-requiring transmembrane kinase/endoribonuclease 1α; ITT, insulin tolerance test; JNK, c-Jun N-terminal kinase; KO, knockout; mRNA, messenger RNA; PBA, 4-phenylbutyric acid; PERK, protein kinase R-like endoplasmic reticulum kinase; PI, propidium iodide; PKA, protein kinase A; RT-qPCR, reverse-transcription quantitative polymerase chain reaction; TG, triglyceride; TUDCA, tauroursodeoxycholic acid; TUNEL, terminal deoxynucleotidyl transferase–mediated deoxyuridine triphosphate nick-end labeling; WT, wild-type.**

Most current article

2352-345X
https://doi.org/10.1016/j.jcmgh.2022.10.002

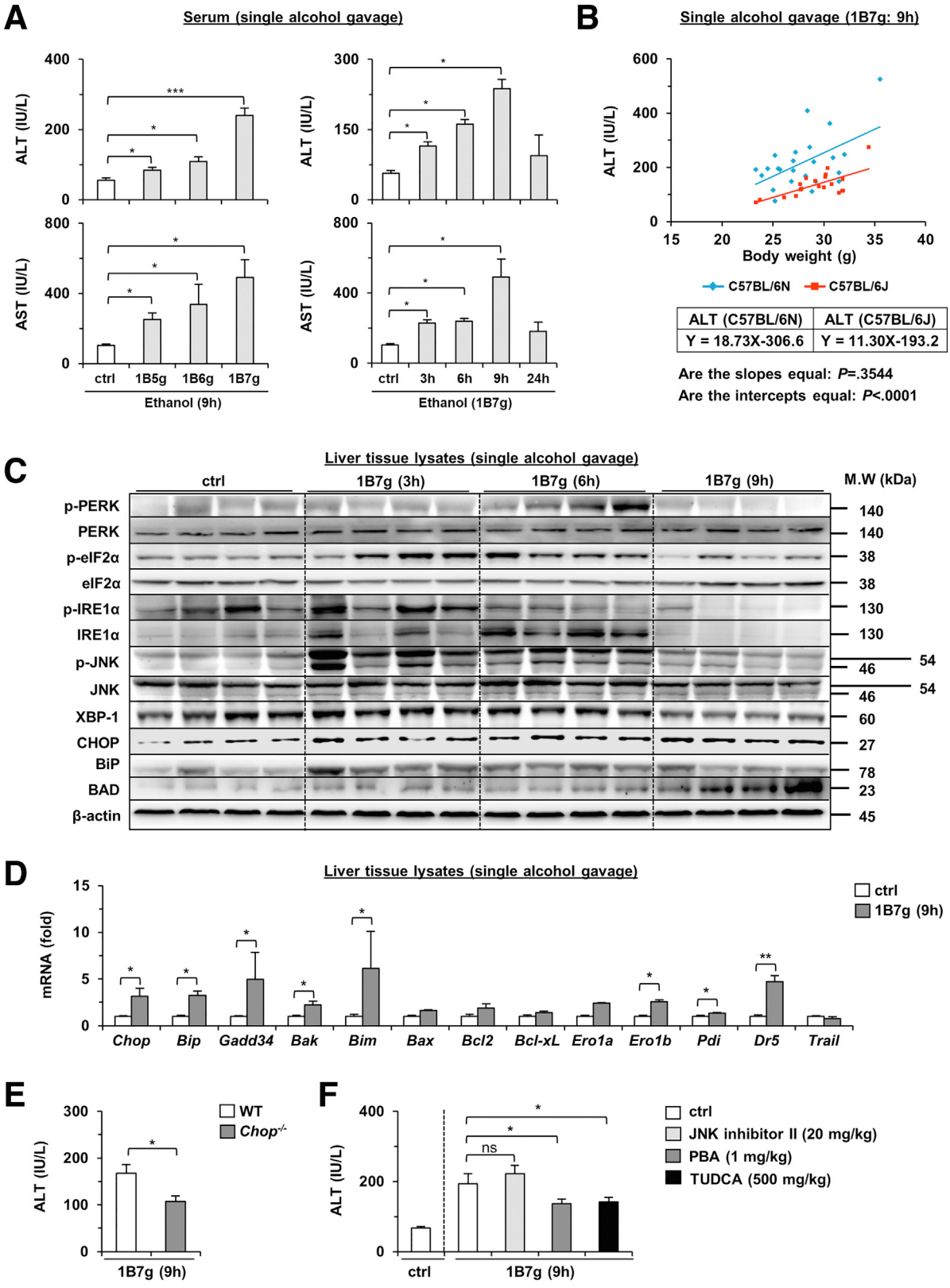

Figure 1. Binge alcohol induces acute liver injury by activating ER stress. C57BL/6N mice (age, 8–10 wk; male) were acutely gavaged with different doses of ethanol (5-7 g/kg). After ethanol gavage, mice were killed at different time points. (*A*) Serum ALT and AST levels were assessed. (*B*) Serum ALT levels in C57BL/6N and C57BL/6J mice were measured after an acute ethanol gavage (7 g/kg ethanol). Liver tissues were subjected to (*C*) Western blot and (*D*) RT-qPCR analysis. (*E*) Serum ALT levels were determined after a single alcohol gavage (7 g/kg) was administered to WT and *Chop*$^{-/-}$ mice (9 hours after alcohol gavage). (*F*) C57BL/6N mice were administered via intraperitoneal injection JNK inhibitor II or ER stress inhibitors, PBA and TUDCA, 15 minutes before 7-g/kg ethanol gavage. Serum ALT levels were measured. Data are expressed as the means ± SEM. *$P < .05$, **$P < .01$, and ***$P < .001$ vs the corresponding controls. ctrl, control; MW, molecular weight.

serum alanine aminotransferase (ALT) (~220 IU/L) and aspartate aminotransferase (AST) (~400 IU/L) was observed in mice receiving 7 g/kg of ethanol approximately 9 hours after administration (Figure 1*A*). We found a positive correlation between body weight and serum ALT levels at 9 hours after a single ethanol binge (7 g/kg) in both C57BL/6N and C57BL/6J mice (Figure 1*B*). However, the increase of serum ALT levels was higher in C57BL/6N mice than in C57BL/6J mice after a single binge (7 g/kg), suggesting that C57BL/6N mice were more sensitive to acute alcoholic injury than C57BL/6J mice (Figure 1*B*). In addition, our data showed that male mice were more susceptible to acute alcohol-induced liver injury than female mice (serum ALT level, ~220 IU/L in male mice vs ~160 IU/L in female mice). Alcohol-induced liver injury also was observed in BALB/c mice, again in a dose-dependent manner with higher serum AST and ALT levels in 7-g/kg ethanol–treated than in 5-g/kg ethanol–treated BALB/c mice (ALT level, ~250 IU/L; AST level, ~340 IU/L in the 7-g/kg binge group vs ALT level, ~125 IU/L; AST level, ~180 IU/L in the 5-g/kg binge group).

Activation of the endoplasmic reticulum (ER) stress pathway has been implicated in ethanol-induced liver injury after chronic ethanol feeding or chronic-plus-binge ethanol feeding.[28] We next asked if the pathway related to liver injury after a single ethanol binge also is attributed to ER stress. As illustrated in Figure 1*C*, a single ethanol binge (7 g/kg) rapidly up-regulated the expression of several ER stress-related proteins, notably phosphorylated Protein kinase-like endoplasmic reticulum kinase (PERK), phosphorylated eukaryotic initiation factor 2 alpha (eIF2α), Inositol-requiring enzyme 1 alpha (IRE1α), phosphorylated c-Jun N-terminal kinase (JNK), C/EBP-homologous protein (CHOP), and Binding immunoglobulin protein (BiP), with the peak expression approximately 3–6 hours after binge. Along with the induction of ER stress-related proteins, hepatic expressions of pro-apoptotic protein such as BCL2 associated agonist of cell death (BAD) (Figure 1*C*), and messenger RNA (mRNA) expressions of *Gadd34*, *Bak*, *Bim*, *Ero1b*, and *Dr5* were increased markedly after a single ethanol binge (Figure 1*D*).

CHOP is induced by ER stress and mediates cellular apoptosis.[29] To confirm that the ER stress pathway is crucial in the pathogenesis of liver injury in a single ethanol binge model, we used a loss-of-function approach using *Chop*$^{-/-}$ mice and the ER stress inhibitors 4-phenylbutyric acid (PBA) and tauroursodeoxycholic acid (TUDCA). The serum ALT levels in *Chop*$^{-/-}$ mice receiving a single ethanol binge at 7 g/kg were markedly lower than those in wild-type (WT) controls (Figure 1*E*). In addition, the administration of ER stress inhibitors (PBA and TUDCA) but not a JNK inhibitor significantly attenuated serum ALT levels in mice receiving a single ethanol binge (Figure 1*F*). Taken together, these data suggest that a single ethanol binge induces hepatocyte injury via the induction of ER stress.

Disruption of the Oxidative Metabolizing Enzyme, Adh1, Exacerbates Acute Ethanol-Induced Liver Injury in Chow- and High-Fat Diet–Fed Mice

To examine whether ethanol or its oxidative metabolites play an important role in alcohol-induced liver injury in our single ethanol binge model, we performed the experiments in mice lacking *Adh1*, a key oxidizing enzyme converting ethanol to acetaldehyde. As expected, blood ethanol concentrations were much higher in *Adh1*$^{-/-}$ mice than in WT mice, notably at 6 and 9 hours after an ethanol binge, whereas the level of serum acetaldehyde was comparable in *Adh1*$^{-/-}$ and WT mice (Figure 2*A*). Interestingly, a single ethanol binge induced higher serum ALT levels in *Adh1*$^{-/-}$ mice than those in WT mice (Figure 2*A*). In agreement with this finding, hepatocyte death, hepatic ER stress-related proteins and genes were higher in *Adh1*$^{-/-}$ mice than those in WT mice after a single ethanol binge (Figure 2*B*–*D*).

In addition to ADH, ethanol can be oxidized by a microsomal ethanol oxidizing system, CYP2E1, and peroxisomal catalase.[9] We therefore performed the experiments to determine the potential role of CYP2E1 and catalase in ALD after a single ethanol binge. There was no difference in the level of serum ALT in WT and *Cyp2e1*$^{-/-}$ mice receiving a single ethanol binge. Treatment with the catalase inhibitor 3-amino-1,2,4-triazole or salicylic acid slightly, but not significantly, increased serum ALT levels in ethanol-treated mice (data not shown). Moreover, binge alcohol intake increased hepatic Malondialdehyde (MDA) levels, however, significant differences between WT and *Adh1*$^{-/-}$ mice were not observed in MDA, *Sod1*, *Sod2*, *catalase*, or several inflammatory markers (data not shown). Collectively, these data suggest that among alcohol-metabolizing enzymes, ADH1, but not CYP2E1 and catalase, plays an important role in acute liver injury in a single ethanol binge model via the inhibition of ER stress, but not oxidative stress.

As previously stated, binge drinking, in combination with metabolic syndrome or obesity, causes a synergistic effect for ALD.[7,8] Next, we further explored whether the deficiency of *Adh1* is also more susceptible to acute alcoholic liver injury under a high-fat diet (HFD)-mediated obese condition. WT and *Adh1*$^{-/-}$ mice fed with a HFD for 3 months without alcohol gavage had similar body weight gain and glucose homeostasis, as measured by the glucose tolerance test (GTT) and the insulin tolerance test (ITT) (Figure 3*A*). Because oral administration of 6 or 7 g/kg ethanol caused high mortality in HFD-fed mice, we only used 5 g/kg ethanol gavage in HFD-fed mice in the following experiments. As illustrated in Figure 3*B*, HFD-fed *Adh1*$^{-/-}$ mice receiving a single ethanol binge had higher levels of blood ethanol concentrations and serum ALT compared with HFD-fed WT mice. However, blood acetaldehyde levels were comparable between WT and *Adh1*$^{-/-}$ mice after a single ethanol binge (Figure 3*B*). Furthermore, HFD-plus-binge ethanol-fed *Adh1*$^{-/-}$ mice had greater liver fibrogenic response and hepatocyte death as shown by H&E, Sirius Red, and terminal deoxynucleotidyl transferase–mediated deoxyuridine triphosphate nick-end labeling (TUNEL) staining, compared with that of WT mice (Figure 3*C*), and higher levels of ER stress and fibrotic genes as shown by reverse-transcription quantitative polymerase chain reaction (RT-qPCR) analyses (Figure 3*D*). Finally, we also performed in vitro experiments in primary hepatocytes isolated from WT and *Adh1*$^{-/-}$ mice treated with palmitic acid (200 μmol/L) in the presence and absence of ethanol (100 mmol/L). We found that mRNA

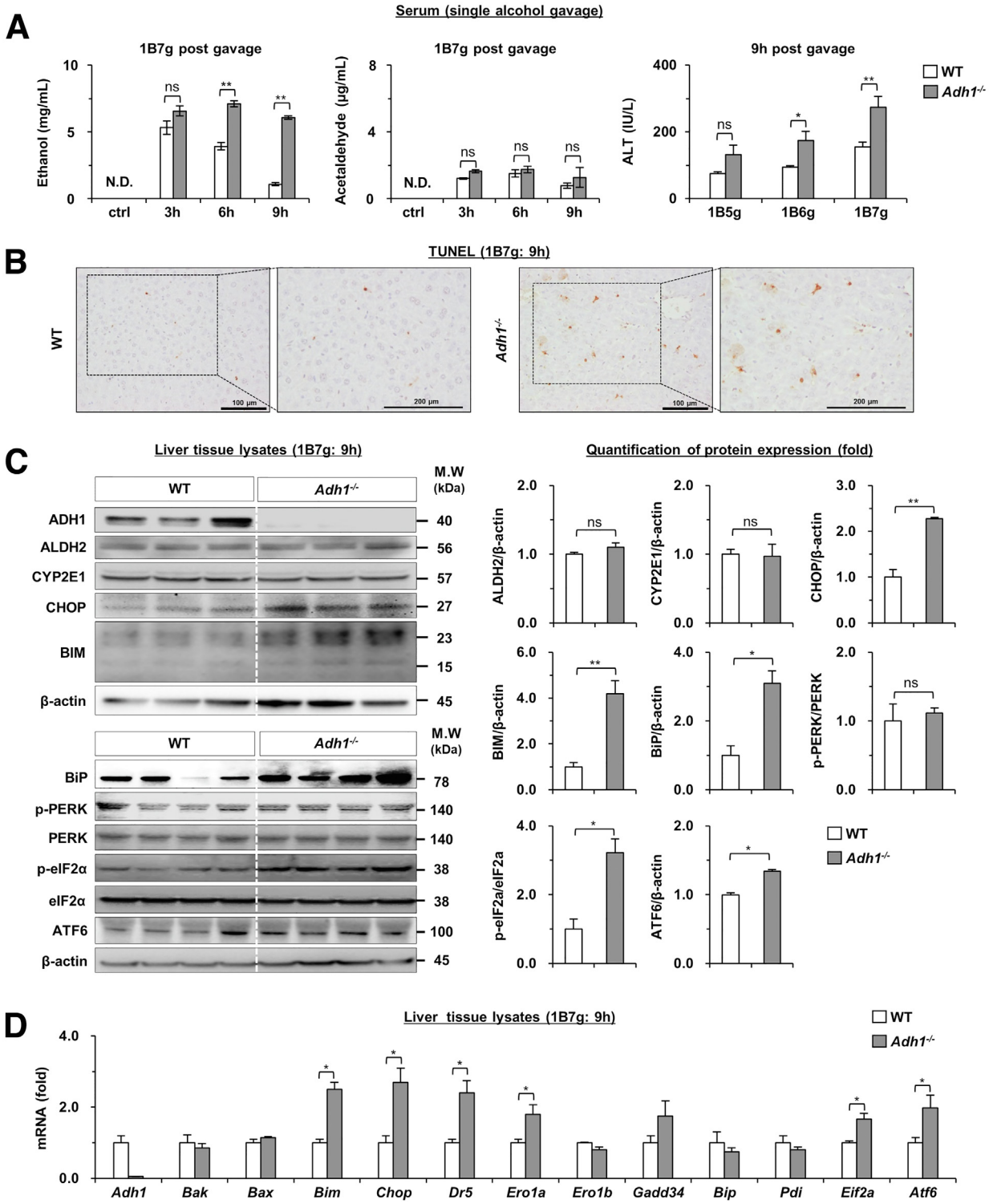

Figure 2. Deletion of the *Adh1* gene exacerbates acute alcoholic liver injury and ER stress–mediated hepatocyte death. Chow-fed WT and *Adh1*$^{-/-}$ mice were given a single ethanol binge. Mice were killed at different time points postgavage. (*A*) Serum ethanol, acetaldehyde, and ALT levels were evaluated. (*B*) Liver tissue sections were subjected to TUNEL staining. Representative images are shown. (*C*) Western blot analyses were performed on liver tissue lysates, and the density of bands was quantified. (*D*) Liver tissues were subjected to RT-qPCR analysis. Data are expressed as the means ± SEM. $^{*}P < .05$, $^{**}P < .01$ vs the corresponding controls. ctrl, control; MW, molecular weight.

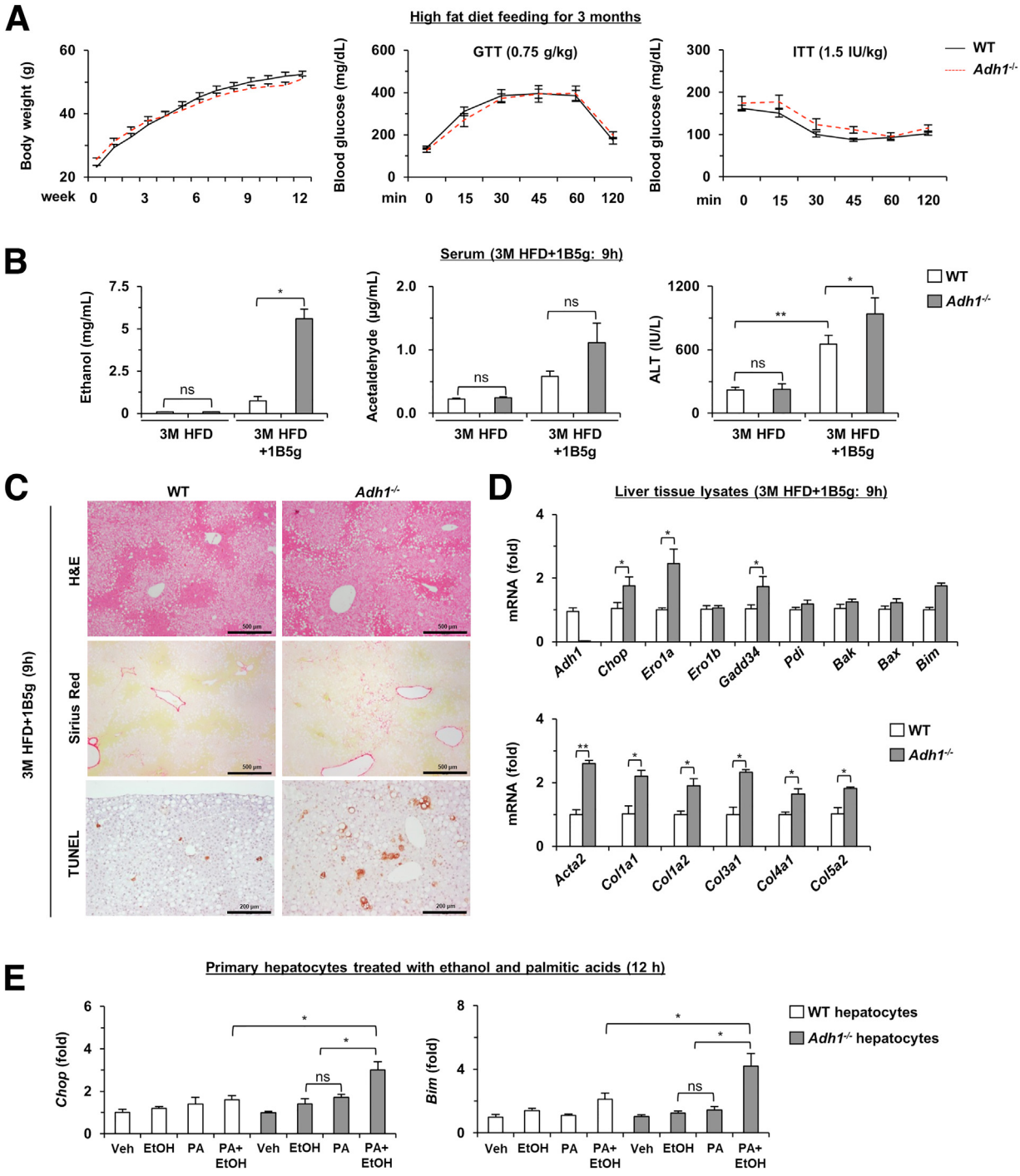

Figure 3. HFD-fed *Adh1*$^{-/-}$ mice are more susceptible to acute alcoholic liver injury and ER stress. (*A*) *Adh1*$^{-/-}$ and WT mice were fed a HFD for 3 months without ethanol binge. Body weight change was evaluated. A GTT (0.75 g/kg glucose via intraperitoneal injection) and an ITT (1.5 IU/kg insulin via intraperitoneal injection) were performed. (*B–D*) *Adh1*$^{-/-}$ and WT mice were fed a HFD for 3 months followed by receiving a single alcohol gavage (5 g/kg) or isocaloric maltose. (*B*) Mice were killed 9 hours after acute alcohol administration. Serum ethanol, acetaldehyde, and ALT levels were measured. (*C*) H&E, Sirius Red, and TUNEL staining were performed on liver tissue sections. (*D*) Liver tissue lysates were subjected to RT-qPCR analysis. (*E*) Freshly isolated hepatocytes (WT and *Adh1*-deficient hepatocytes) were treated with palmitic acid (200 μmol/L) and ethanol (100 mmol/L) for 12 hours, followed by performing RT-qPCR. Data are expressed as the means ± SEM. *$P < .05$, **$P < .01$ vs the corresponding controls. PA, palmitic acid; Veh, vehicle; 3M, 3-months.

expression of *Chop* and *Bim* was significantly higher in *Adh1*-deficient hepatocytes treated with both palmitic acid and ethanol when compared with those treated with either palmitic acid or ethanol (Figure 3*E*).

Depletion of the Oxidative Metabolizing Enzyme Aldh2 Does Not Exaggerate Acute Alcohol-Induced Liver Injury in Chow-Fed and HFD-Fed Mice

Once generated from the metabolism of alcohol by oxidative enzymes, acetaldehyde subsequently is converted to acetate by ALDH2. To evaluate the role of acetaldehyde in a single binge ethanol model, we performed the experiments using *Aldh2*$^{-/-}$ mice. Administration of ethanol at 7 g/kg caused significantly high mortality in *Aldh2*$^{-/-}$ mice; we therefore used 6 g/kg ethanol in *Aldh2*$^{-/-}$ mice and their controls in the subsequent experiments. After ethanol gavage, blood ethanol concentrations were slightly but significantly higher in *Aldh2*$^{-/-}$ than those in WT mice, whereas much higher blood acetaldehyde levels were observed in *Aldh2*$^{-/-}$ mice than in WT mice after ethanol gavage (Figure 4*A*). Despite higher levels of acetaldehyde, the serum ALT levels in *Aldh2*$^{-/-}$ and WT mice were comparable, suggesting that high blood acetaldehyde does not play a significant role in alcohol-induced liver injury in our model (Figure 4*A*). Hepatic expression of several ER stress-related genes, except for *Gadd34* (DNA damage-inducible gene), also was similar between both groups after ethanol gavage (Figure 4*B*). Protein expressions of CYP2E1 and ER stress-related proteins CHOP and Bcl-2 Interacting Mediator of cell death (BIM), also were similar between both groups after a single ethanol gavage (Figure 4*C*).

We also explored the involvement of ALDH2 on liver injury induced by ethanol binge in combination with the HFD feeding. *Aldh2*$^{-/-}$ mice had similar body weight gains and glucose homeostasis, as measured by the GTT and ITT when compared with corresponding WT groups after 3 months of HFD feeding without ethanol gavage (Figure 5*A*). After ethanol gavage (5 g/kg), HFD-fed *Aldh2*$^{-/-}$ mice had much higher levels of blood acetaldehyde levels compared with WT mice, but both groups had similar serum ALT levels (Figure 5*B*), hepatocyte death, hepatic collagen deposition, and hepatic expression of ER stress and fibrotic genes (Figure 5*C*).

Administration of Ethanol, but Not Acetaldehyde, Induces Liver Injury by Promoting ER Stress and Hepatocyte Death

To further determine whether ethanol or acetaldehyde induces acute liver injury in a single binge ethanol model, ethanol or acetaldehyde was administered via an intraperitoneal route to WT mice. As illustrated in Figure 6*A*, the intraperitoneal administration of ethanol (6 g/kg) rapidly increased blood ethanol levels (left panel) and serum ALT levels (right panel). Hepatic expression of ER stress-related genes (*Chop* and *Xbp-1*), cell death–associated genes (*Bim*, *Bax*, and *Bak*), and neutrophil infiltration–related genes (*Ly6g*, *Lcn2*, and *Cxcl1*) were up-regulated with the peak induction at 9 hours after administration (Figure 6*B*). Next, we also administered ethanol intraperitoneally to WT and *Adh1*$^{-/-}$ mice and killed them 9 hours after administration. As illustrated in Figure 6*C*, serum ALT and ethanol levels, but not acetaldehyde, were higher in *Adh1*$^{-/-}$ mice compared with corresponding WT mice. Concomitantly, hepatic expressions of *Chop*, *Xbp-1*, and *Bim* were greater in *Adh1*$^{-/-}$ mice than in WT mice (Figure 6*C*).

Next, we also evaluated the involvement of acetaldehyde in acute liver injury by intraperitoneal injection of acetaldehyde (50 mg/kg). As illustrated in Figure 6*D*, injection of acetaldehyde rapidly increased blood acetaldehyde levels with the peak at 15 minutes after injection; its level gradually decreased to very low levels at 3 hours after injection, which is probably because acetaldehyde is short-lived and metabolized rapidly in the liver. Administration of acetaldehyde slightly increased serum ALT levels for up to 1 hour, but it did not reach a statistical difference, suggesting that acetaldehyde does not attribute to acute liver injury (Figure 6*D*).

Acute Alcohol Gavage Increases Hepatic Expression of Fatty Acid Synthesis–Related Genes, Increases Serum Free Fatty Acids, and Increases Adipose Tissue Lipolysis

To understand molecular mechanisms of acute liver injury after a single ethanol binge, we subjected liver tissues for microarray analyses and analyzed lipid metabolism–associated gene expression profiles. A large number of dysregulated genes was observed in the livers of mice receiving 5 or 7 g/kg ethanol gavage compared with those from control mice, with the most alternations from the 7 g/kg ethanol gavage group (Figure 7*A*). The genes related to fatty acid metabolism were the most altered in mice receiving 7 g/kg ethanol gavage compared with controls and those receiving a 5 g/kg ethanol gavage (Figure 7*B* and *C*). In more details, oral administration of 7 g/kg ethanol markedly up-regulated hepatic expression of de novo lipogenesis genes (*Acaca*, *Fasn*, and *Cyp51*), but attenuated hepatic expression of the fatty acid oxidation pathway (*Pparα*, *Fgf21*, and *Cyp4a10*), with limited impact on hepatic triglyceride (TG) synthesis (*Dgat2* and *Ldlr*) (Figure 8*A*). Interestingly, lipid droplet dynamics–related genes (*Apoe* and *Apob*) also were altered with acute alcohol gavage. In addition, the administration of 7 g/kg alcohol was highly associated with proinflammatory responses and inversely associated with fatty acid oxidation (Figure 8*A*).

To further explore how 7 g/kg ethanol gavage induces acute liver injury and how fatty acid metabolism is involved, we measured serum and hepatic free fatty acids (FFAs) and hepatic TG levels. As illustrated in Figure 8*B*, oral administration of 7 g/kg ethanol markedly increased serum and hepatic FFAs as well as hepatic triglyceride levels. In addition, hepatic levels of several FFAs including palmitic acid, oleic acid, and linoleic acid were increased drastically after oral alcohol administration (Figure 8*C*). Hepatic expressions of fatty acid synthase (FASN) and stearoyl-CoA desaturase 1

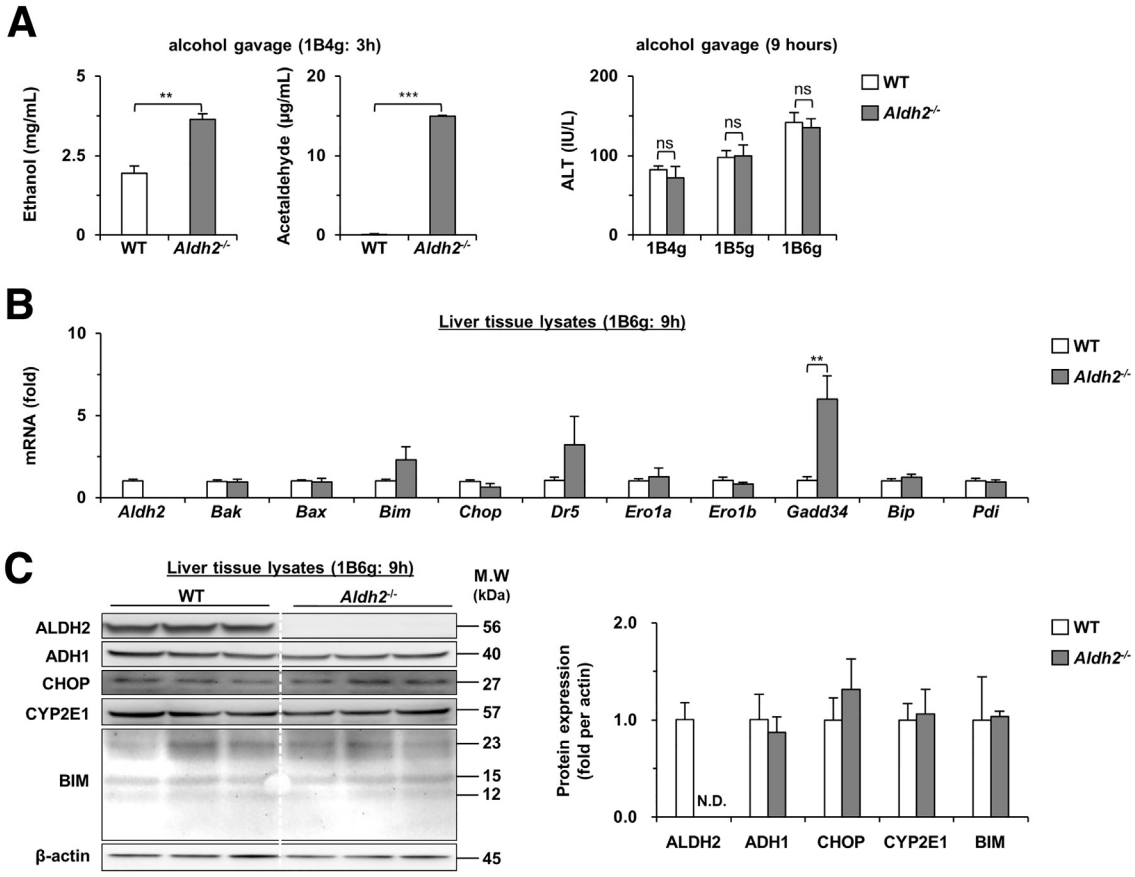

Figure 4. Deletion of the *Aldh2* gene does not affect acute alcoholic liver injury. (*A*) *Aldh2*$^{-/-}$ and WT mice were subjected to ethanol gavage (4 g/kg of ethanol) and killed 3 hours after gavage. Blood ethanol and acetaldehyde levels were measured. In addition, *Aldh2*$^{-/-}$ and WT mice were subjected to ethanol gavage (various doses of ethanol) and killed 9 hours postgavage, followed by measuring serum ALT levels. (*B* and *C*) *Aldh2*$^{-/-}$ and WT mice were subjected to ethanol gavage (6 g/kg of ethanol) and killed 9 hours after gavage. RT-qPCR and Western blot analyses were performed on liver tissue lysates. Data are expressed as the means ± SEM. $^{**}P < .01$, and $^{***}P < .001$ vs the corresponding controls. MW, molecular weight.

(SCD1) proteins, which play an important role in fatty acid synthesis, were highly up-regulated after acute alcohol gavage (Figure 8*C*).

Because serum levels of FFAs were highly increased after a single ethanol binge, and adipose lipolysis has been shown to promote steatosis,[20] we wondered whether adipose tissue is the source of circulating FFAs through the lipolytic process in the adipose tissues. To test this hypothesis, we performed Western blot analyses of lipolysis-related proteins. Our data show that oral ethanol administration increased the expression of lipolysis proteins such as phosphorylated protein kinase A (PKA), phosphorylated hormone-sensitive lipase (HSL), and adipose triglyceride lipase in adipose tissues, suggesting acute alcohol gavage–induced adipose tissue lipolysis (Figure 8*D*).

Acute Alcohol Gavage Causes Adipocyte Death and ER Stress in Adipose Tissues, Which Is Enhanced in Adh1$^{-/-}$ *but Not in* Aldh2$^{-/-}$ *Mice*

We previously showed that adipocyte death triggers lipolysis.[30] Thus, we speculated whether acute ethanol-induced lipolysis was the result of induction of adipocyte death. To answer this question, we measured ethanol and acetaldehyde concentrations in adipose and liver tissues after ethanol gavage. As illustrated in Figure 9*A*, total ethanol concentrations were comparable between the liver and adipose tissues after ethanol gavage except for the 1-hour time point in which ethanol concentrations were higher in the liver than in adipose tissues, and the levels of acetaldehyde were much lower in adipose tissues than in liver tissues after a single binge (Figure 9*A*).

Next, we examined adipose tissue histology after a single ethanol gavage. Our preliminary data showed that the number of crown-like structures (CLSs) was higher in epididymal fat than in subcutaneous fat after alcohol gavage (both single binge and 3 months HFD-plus-binge). In addition, we did not observe significant morphologic changes/gene expression of brown adipose tissues in the single binge model and the HFD-plus-binge ethanol feeding model compared with their corresponding controls (data not shown). Thus, we focused on epididymal fat in this study and found that epididymal adipose tissues had an increase in CLS after a single ethanol binge compared with the control group, and the number of TUNEL^{+}

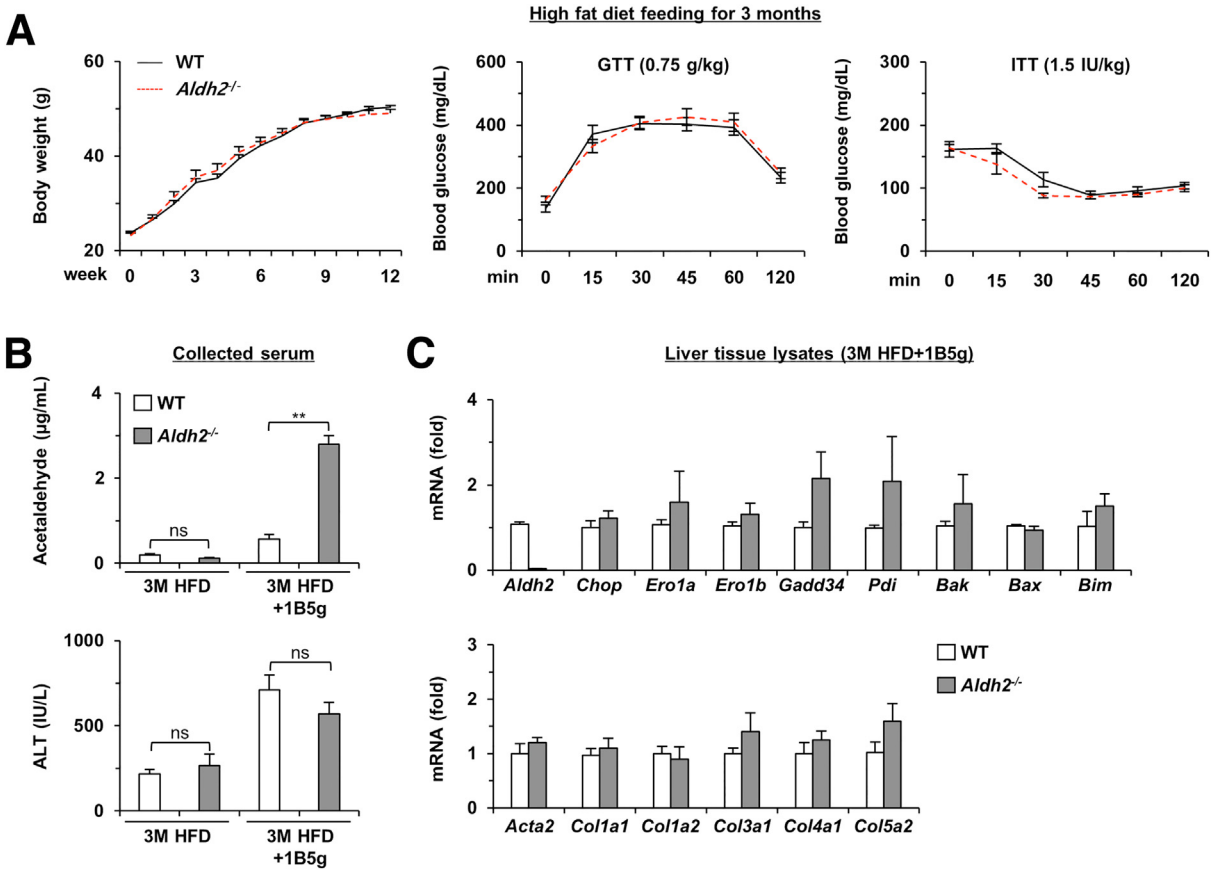

Figure 5. Deletion of the *Aldh2* gene does not exacerbate acute alcoholic liver injury, obesity, and insulin resistance. (*A*) *Aldh2*$^{-/-}$ and WT mice were fed a HFD for 3 months without ethanol gavage. Body weight change, GTT (0.75 g/kg glucose via intraperitoneal injection), and ITT (1.5 IU/kg insulin via intraperitoneal injection) were evaluated. (*B* and *C*) *Aldh2*$^{-/-}$ and WT mice were fed a HFD for 3 months followed by a single dose of ethanol (5 g/kg) or isocaloric maltose, and the mice were killed 9 hours later. (*B*) Serum acetaldehyde and ALT levels were assessed. (*C*) Liver tissue lysates were subjected to RT-qPCR analysis. Data are expressed as the means ± SEM. $^{**}P < .01$ vs the corresponding controls. 3M, 3 months.

and F4/80^{+} cells was increased mostly around the CLS after ethanol gavage (Figure 9*B*), showing a typical pattern of adipocyte death formed by the accumulation of macrophages around the dead/injured adipocytes. Caspase 3/7 activity was increased in the binge alcohol gavage group compared with the control group (Figure 9*C*). Furthermore, RT-qPCR data showed that the expression of several ER stress–related genes in adipose tissues was up-regulated after acute alcohol gavage (Figure 9*C*).

We further explored acute alcohol-induced adipocyte death and lipolysis in *Adh1*$^{-/-}$ mice. Figure 9*D* shows that adipose tissues from *Adh1*$^{-/-}$ mice had a greater number of the CLS and TUNEL^{+} cells. As expected, *Adh1*$^{-/-}$ mice had higher levels of ethanol and caspase 3/7 activity, but lower levels of acetaldehyde than WT mice after a single ethanol gavage (Figure 9*E*). The levels of serum FFA, and the expression of ER stress–, cell death–, and lipolysis-related genes in adipose tissues were greater in *Adh1*$^{-/-}$ mice compared with WT mice after ethanol gavage (Figure 9*E* and *F*).

In addition, binge alcohol gavage (6 g/kg) was given to *Aldh2*$^{-/-}$ and WT mice. After the binge alcohol gavage, acetaldehyde concentration in white adipose tissues was much higher in *Aldh2*$^{-/-}$ mice than that in WT mice, as we expected (Figure 10*A*). Interestingly, ethanol levels in adipose tissues were also slightly higher in *Aldh2*$^{-/-}$ mice than in WT mice (Figure 10*A*). Despite higher levels of acetaldehyde, *Aldh2*$^{-/-}$ mice showed similar CLS formation, TUNEL^{+} cells, and caspase 3/7 activity (Figure 10*B* and *C*). RT-qPCR analyses revealed the expression of several ER stress–related genes in adipose tissues was higher in *Aldh2*$^{-/-}$ mice compared with WT controls, but the expression of cell death– and lipolysis-related genes tended to increase but was not statistically significant (Figure 10*D*).

Ethanol Directly Induces Adipocyte Death and ER Stress in Cultured Adipocytes

The earlier-described data revealed that a high concentration of ethanol but not acetaldehyde correlates with greater adipocyte death in vivo, suggesting ethanol but not acetaldehyde induces adipocyte death. To investigate the effects of ethanol on adipocyte injury in the in vitro setting, we analyzed adipocyte death by annexin V and propidium iodide (PI) staining. As shown in Figure 11*A*, ethanol exposure to a differentiated adipocyte cell line (3T3-L1) markedly increased annexin-V and PI staining. Furthermore,

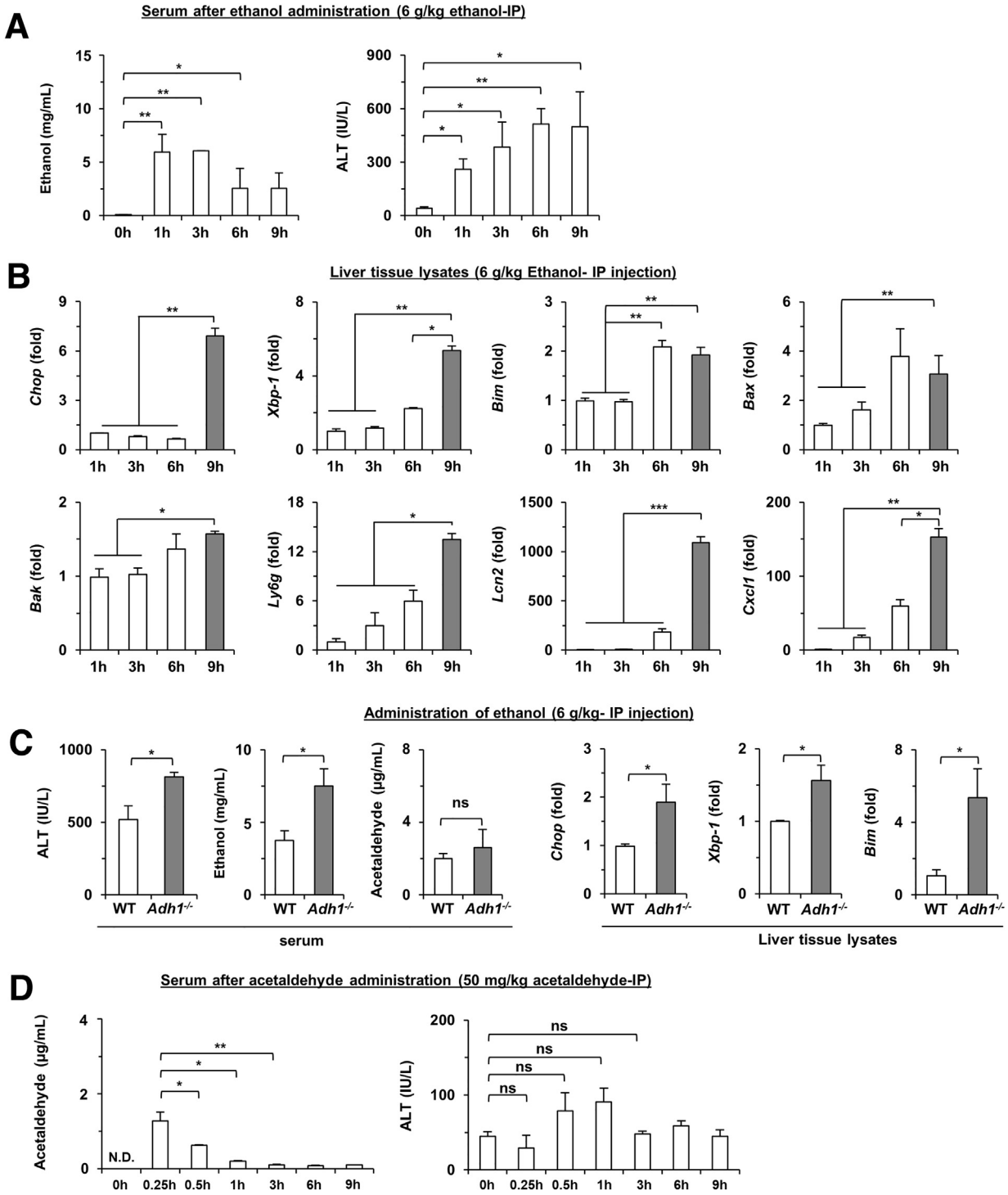

Figure 6. Intraperitoneal administration of ethanol, not acetaldehyde, induces acute liver injury and hepatic ER stress. (*A–C*) C57BL/6N mice were intraperitoneally administered 6 g/kg ethanol and were killed 9 hours postinjection. (*A*) Serum samples of ethanol and ALT levels were measured. (*B*) Liver tissue lysates at different time points were subjected to RT-qPCR analyses. (*C*) Serum and liver tissues from WT and *Adh1*$^{-/-}$ mice were tested for ALT, ethanol, and acetaldehyde levels, as well as hepatic mRNA expression. (*D*) C57BL/6N mice were injected intraperitoneally with acetaldehyde (50 mg/kg) and killed 9 hours later. Serum acetaldehyde and ALT levels were determined. Data are expressed as the means ± SEM. **P* <.05, ***P* < .01, and ****P* < .001 vs the corresponding controls. IP, intraperitoneal.

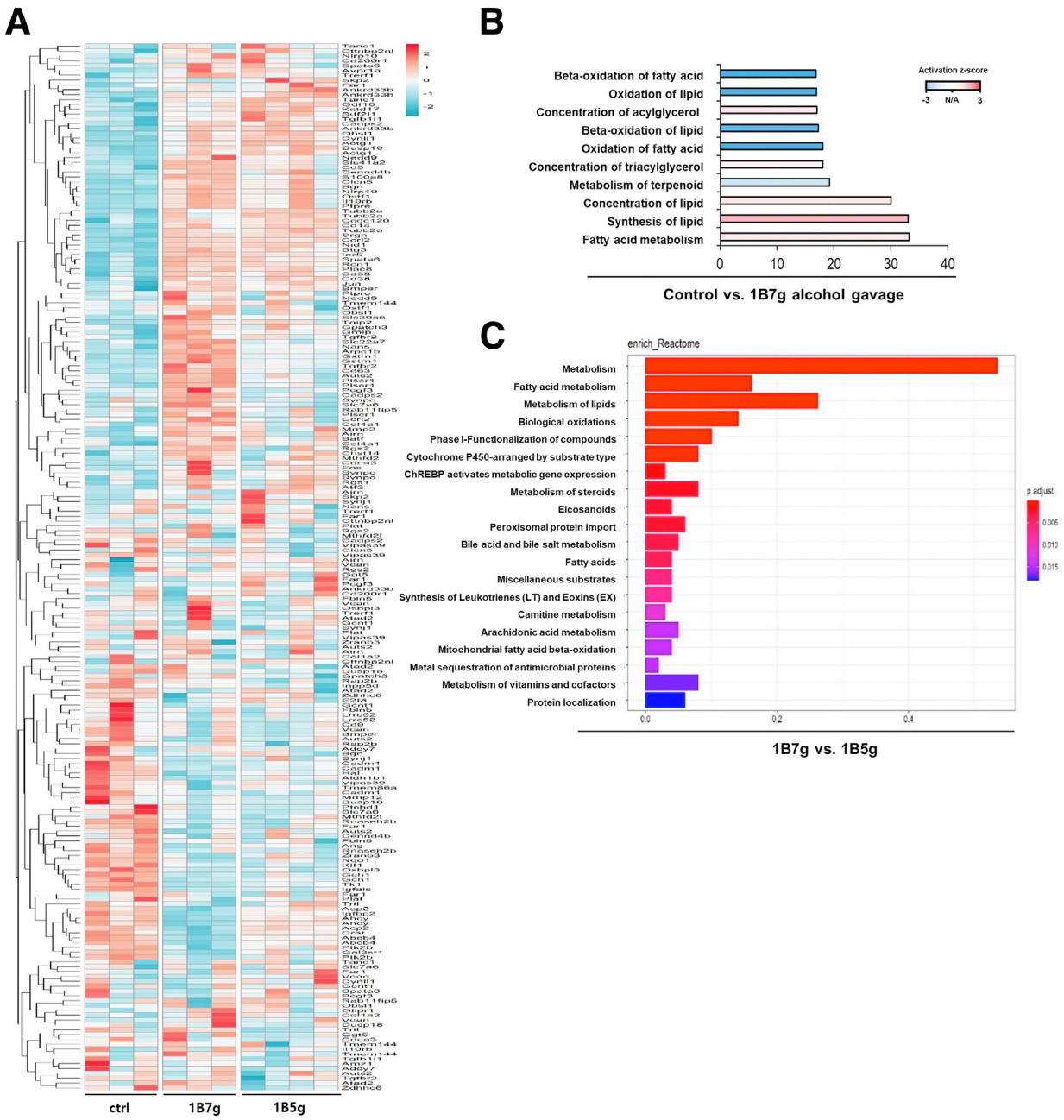

Figure 7. Binge ethanol causes increased lipid synthesis and a decrease in β-oxidation. (*A*) Z-score hierarchical clustering heat map visualization changes are shown. The colors reflect scaled expression levels, with blue representing low expression and red representing high expression. (*B*) Predicted up-regulation/down-regulation of top lipid metabolism functions using biofunctional analysis (control vs 1B7g). (*C*) Ingenuity pathway analysis (IPA) was used to show the top 20 predicted pathways that differed significantly from ethanol binge 5 g/kg vs ethanol binge 7 g/kg. ChREBP, carbohydrate response element binding protein.

ethanol treatment induced adipocyte death as evidenced by an increase of *Cyto c ox* gene copy, DNA fragmentation, and expression of several apoptosis-related genes (Figure 11*B*). To understand the mechanisms by which ethanol induces adipocyte death and lipolysis, we treated the differentiated pre-adipocytes from white adipose tissues with ethanol, and then performed immunoblotting and RT-qPCR analyses for ER stress– and lipolysis-related proteins. As illustrated in Figure 11*C* and *D*, ethanol treatment markedly increased the expression of several ER stress– or lipolysis-related proteins and genes in differentiated adipocytes.

Inhibition of Adipocyte Death Ameliorates Acute Alcohol or Acute-on-Chronic Ethanol-Induced Liver ER Stress and Injury

To examine whether adipocyte death induced by binge alcohol gavage contributes to alcohol-induced lipolysis and

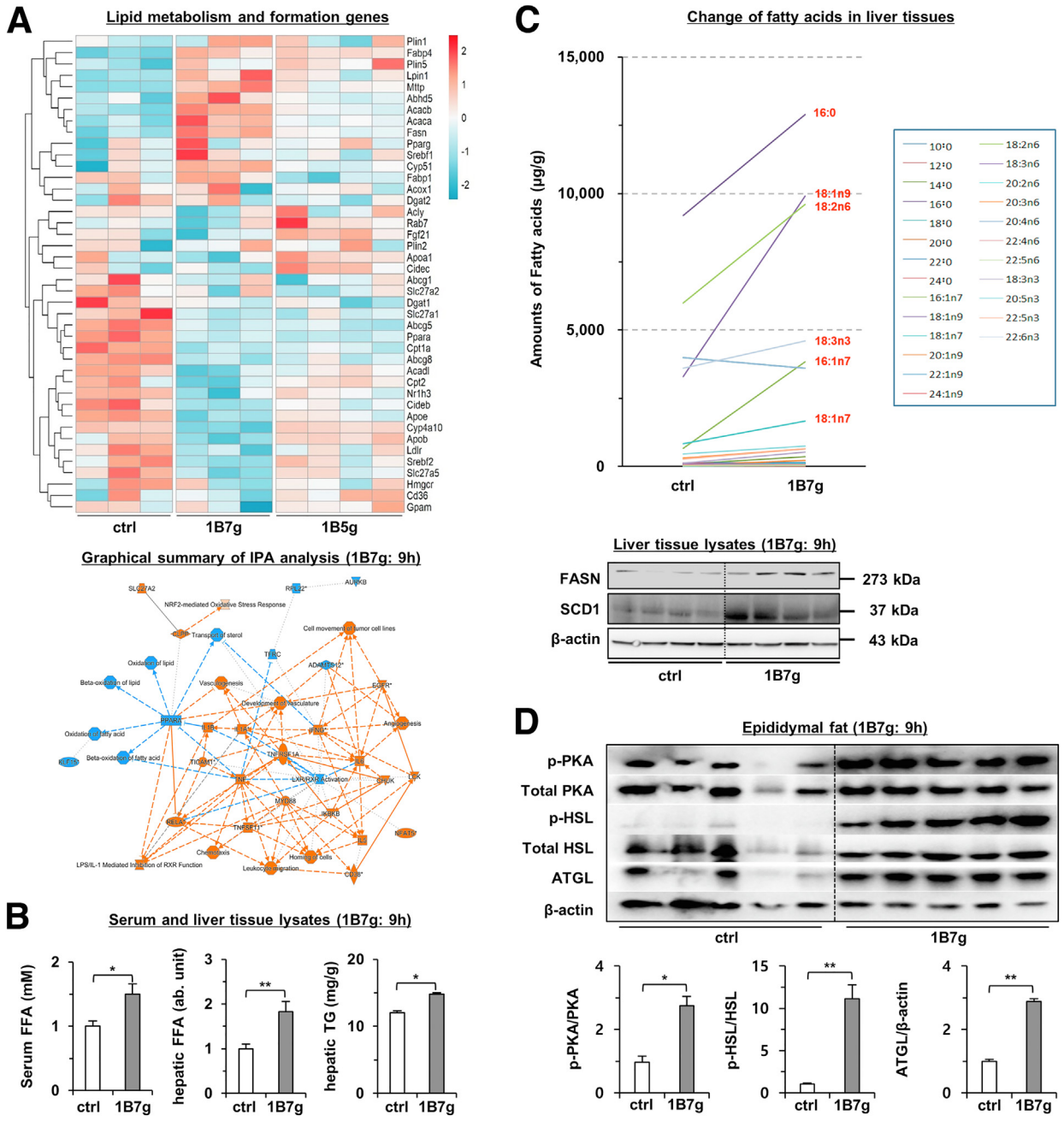

Figure 8. Binge ethanol increases hepatic FFAs and increases adipose tissue lipolysis. Mice were subjected to a single ethanol binge (5 or 7 g/kg) or isocaloric maltose and were killed 9 hours after alcohol gavage. (*A*) Liver tissues were subjected to microarray analyses. The heatmap and ingenuity pathway analysis (IPA) analyses for liver mRNA expression are shown. (*B*) Sera were collected for FFA measurement. Liver FFA and TG levels were measured. (*C*) Gas chromatography–mass spectrometry was used to perform specific FFA studies on liver tissues. Hepatic FASN and SCD1 proteins were analyzed using Western blot. (*D*) Collected white adipose tissues was analyzed using Western blot. Data are expressed as the means ± SEM. $^{*}P < .05$, $^{**}P < .01$ vs the corresponding controls. ctrl, control.

liver injury, we developed adipocyte-specific *Bcl2* transgenic mice ($Bcl2^{AdipoTg}$) in which anti-apoptotic BCL2 protein was specifically overexpressed in adipose tissue. $Bcl2^{AdipoTg}$ mice had less adipocyte death after ethanol gavage, as evidenced by reduction of CLS formation and $TUNEL^{+}$ cells, and lower caspase 3/7 activity compared with WT mice (Figure 12*A* and *B*). Less adipocytes death in $Bcl2^{AdipoTg}$ mice correlated with reduced adipocyte lipolysis in these mice, as indicated by down-regulated expression of lipolysis-related genes (Figure 12*B*) and decreased serum FFA levels (Figure 12*C*). Blood ethanol and acetaldehyde levels were comparable between $Bcl2^{AdipoTg}$ and WT mice after a single ethanol

gavage (Figure 12*C*). We further examined acute alcoholic liver injury in *Bcl2*^{AdipoTg} and WT mice. Serum ALT levels, hepatic TG levels, and hepatic mRNA expression of several lipid metabolism–, ER stress–, and cell death–related genes were lower in *Bcl2*^{AdipoTg} mice compared with WT mice after ethanol binge (Figure 12*C* and *D*).

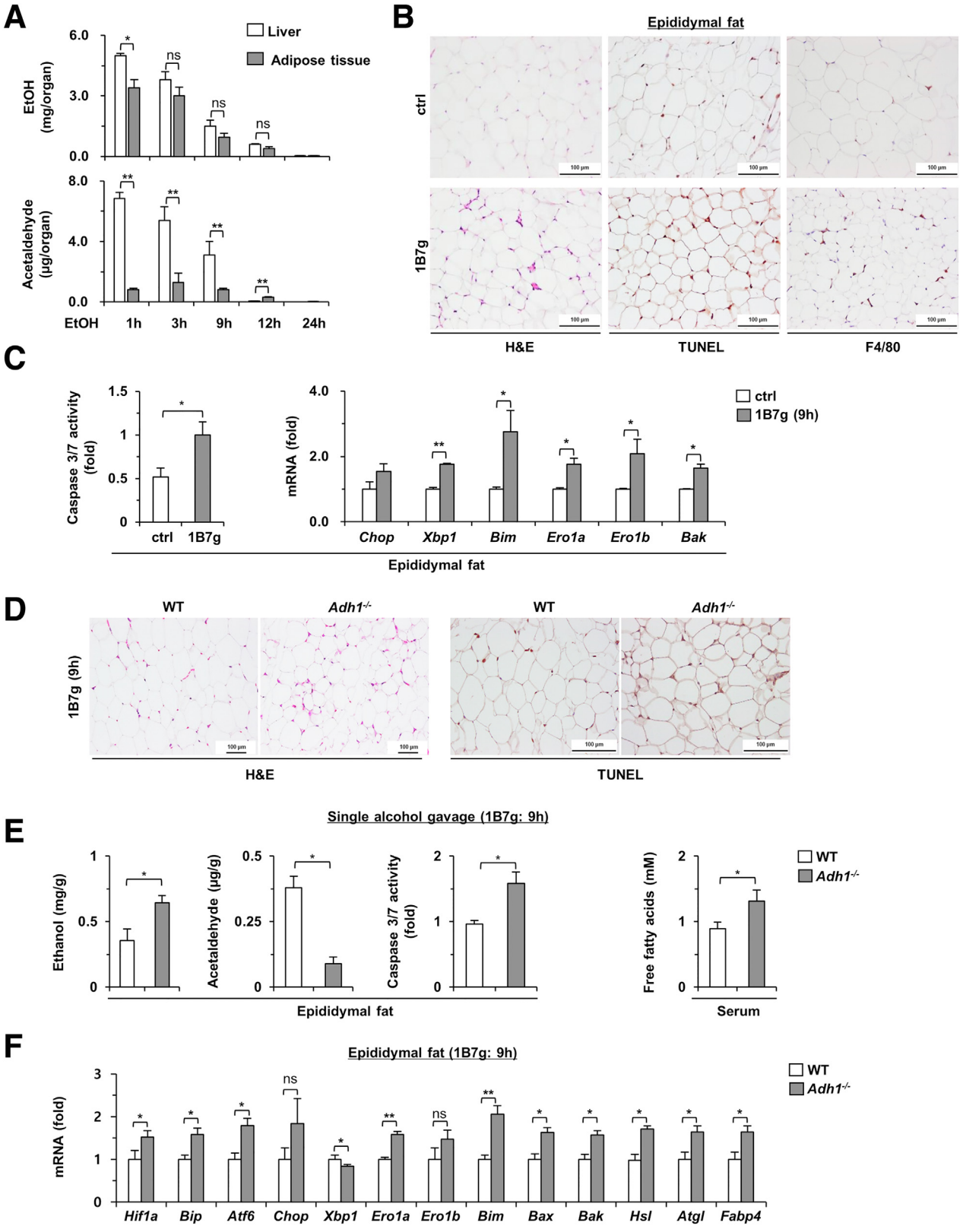

Resistance to ethanol-induced adipocyte death in *Bcl2*^{AdipoTg} mice also was found in an acute-on-chronic ethanol feeding model as shown by the results that *Bcl2*$^{A\text{-}dipoTg}$ mice had lower levels of caspase 3/7 activity in adipose tissues than WT mice after ethanol gavage (Figure 13*A*). *Bcl2*^{AdipoTg} mice had lower levels of serum FFAs and reduced expression of several lipolysis-related genes in adipose tissues (Figure 13*B* and *C*). Furthermore, serum ALT levels and hepatic TG levels were lower in *Bcl2*^{AdipoTg} mice than in WT mice after chronic-plus-binge ethanol feeding (Figure 13*D* and *E*). Hepatic expressions of several ER stress– and DNA damage–related mRNAs/proteins were lower in ethanol-fed *Bcl2*^{AdipoTg} mice compared with WT mice after chronic-plus-binge ethanol feeding (Figure 13*F* and *G*).

To further explore the effect of adipocyte death on alcohol-induced liver injury, we also used *Bcl-xL* adipocyte-specific knockout (KO) mice. After acute-on-chronic ethanol feeding, *Bcl-xL*^{AdipoKO} mice showed increased adipocyte death (higher levels of CLS formation and caspase 3/7 activity in adipose tissue) (Figure 14*A* and *B*) and increased lipolysis (higher expression of lipolysis-related genes in adipose tissue) (Figure 14*C*) compared with WT mice. Serum FFA levels also were higher in *Bcl-xL*^{AdipoKO} mice compared with controls (Figure 14*D*). Furthermore, *Bcl-xL*^{AdipoKO} mice had more steatosis, increased caspase 3/7 activity, and greater expression of several ER stress–related genes in the liver than WT mice after chronic-plus-binge ethanol feeding (Figure 14*E* and *F*). There were no statistical differences in serum ALT levels between *Bcl-xL*^{AdipoKO} and WT mice after chronic-plus-binge ethanol feeding (Figure 14*G*).

Nonoxidative Ethanol Metabolite FAEEs Contribute to Acute Alcohol-Induced Liver Injury

In addition to the oxidative process converting alcohol to acetaldehyde by alcohol-metabolizing enzymes, a nonoxidative alcohol metabolism also has been implicated in the pathogenesis of alcohol-induced organ damage via the production of FAEEs (Figure 15*A*).[31] Our data suggest that acetaldehyde does not play a key role in acute liver injury after a single ethanol binge, so we wondered whether nonoxidative ethanol metabolites, FAEEs, contribute to acute ethanol-induced liver injury. We evaluated serum FAEE levels using gas chromatography with a flame ionization detector, as previously described.[12] After acute alcohol administration, a significant increase in serum FAEEs was observed compared with those in controls (Figure 15*B*). Intriguingly, serum FAEE levels were almost 3 times higher in *Adh1*$^{-/-}$ mice than those in WT mice. The major FAEEs were composed of palmitic acid ethyl ester (16:0 ethyl ester), stearic acid ethyl ester (18:0 ethyl ester), and oleic acid ethyl ester (18:1n9 ethyl ester) (Figure 15*C*). Similarly, *Adh1*$^{-/-}$ mice fed with a HFD for 3 months and a single ethanol binge showed higher levels of FAEEs compared with those in WT mice (Figure 15*C*). Taken together, acute alcohol administration lead to an increase in serum FAEEs, and the inhibition of oxidative alcohol metabolism in *Adh1*$^{-/-}$ mice resulted in an increase in the production of nonoxidative ethanol metabolites in both chow- and HFD-fed mice.

Next, we investigated the hepatic expression of the FAEE synthesis–associated gene *Ces1d*. As shown in Figure 16*A*, the highest expression of *Ces1d* was detected in the liver compared with other organs. In the liver, *Ces1d* was detected mainly in hepatocytes, while its expression was detected at very low levels in other nonhepatic parenchymal cells. To examine the role of *Ces1d* in acute alcohol-induced liver injury, *Ces1d*$^{-/-}$ and WT mice were subjected to a single ethanol binge. Serum levels of ethanol and acetaldehyde were comparable between *Ces1d*$^{-/-}$ and WT mice, while the levels of serum FAEEs were much lower in *Ces1d*$^{-/-}$ mice than in WT mice after acute ethanol gavage (Figure 16*B*). A small reduction in serum ALT levels was observed in ethanol-fed *Ces1d*$^{-/-}$ mice compared with ethanol-fed WT mice, which reached a statistical difference when a large number of mice were used (Figure 16*C*). In addition, the hepatic expression of several ER stress–mediated proteins was lower in *Ces1d*$^{-/-}$ mice than in WT mice (Figure 16*D*). *Cel* is another important FAEE synthesis enzyme to catalyze FAEE synthesis, however, *Cel* mRNA was expressed mainly in the pancreas and hardly detected in the liver.[12] Here, we also found the carboxyl ester lipase (CEL) protein expression was detected at high levels in the pancreas but not in the liver tissues (Figure 16*E*). Deletion of the *Cel* gene did not attenuate acute alcohol-induced liver injury (Figure 16*F*). Taken together, *Ces1d* is highly expressed in hepatocytes and partially contributes to acute alcohol-induced liver injury via FAEE production, while carboxyl ester lipase CEL does not contribute significantly to acute alcohol-induced liver injury.

Figure 9. (***See previous page***). **Binge ethanol induces adipocyte death and ER stress in adipose tissues with greater induction in *Adh1*$^{-/-}$ mice than in WT mice.** (*A–C*) C57BL/6N mice were treated with a single ethanol binge (7 g/kg) or isocaloric maltose and killed at various time points after alcohol gavage. Liver and white adipose tissues were collected for the following analyses. (*A*) Ethanol and acetaldehyde concentrations in liver and white adipose tissues (epididymal fat and subcutaneous fat) were determined. (*B*) Representative staining images of H&E, TUNEL, and F4/80 staining of epididymal fat tissues 9 hours after ethanol gavage. (*C*) Caspase 3/7 activity assays and RT-qPCR analysis of ER stress and lipolysis-associated genes in epididymal fat tissues 9 hours after ethanol gavage were performed. (*D–F*) *Adh1*$^{-/-}$ and WT mice were subjected to 7 g/kg alcohol gavage and killed 9 hours after alcohol administration. (*D*) H&E and TUNEL staining were performed on sections of white adipose tissue. (*E*) Ethanol, acetaldehyde, and caspase 3/7 activity were measured in white adipose tissues. Serum FFA levels were assessed. (*F*) Adipose tissues were subjected to RT-qPCR analyses. Data are expressed as the means ± SEM. **P* < .05, ***P* < .01 vs the corresponding controls. ctrl, control.

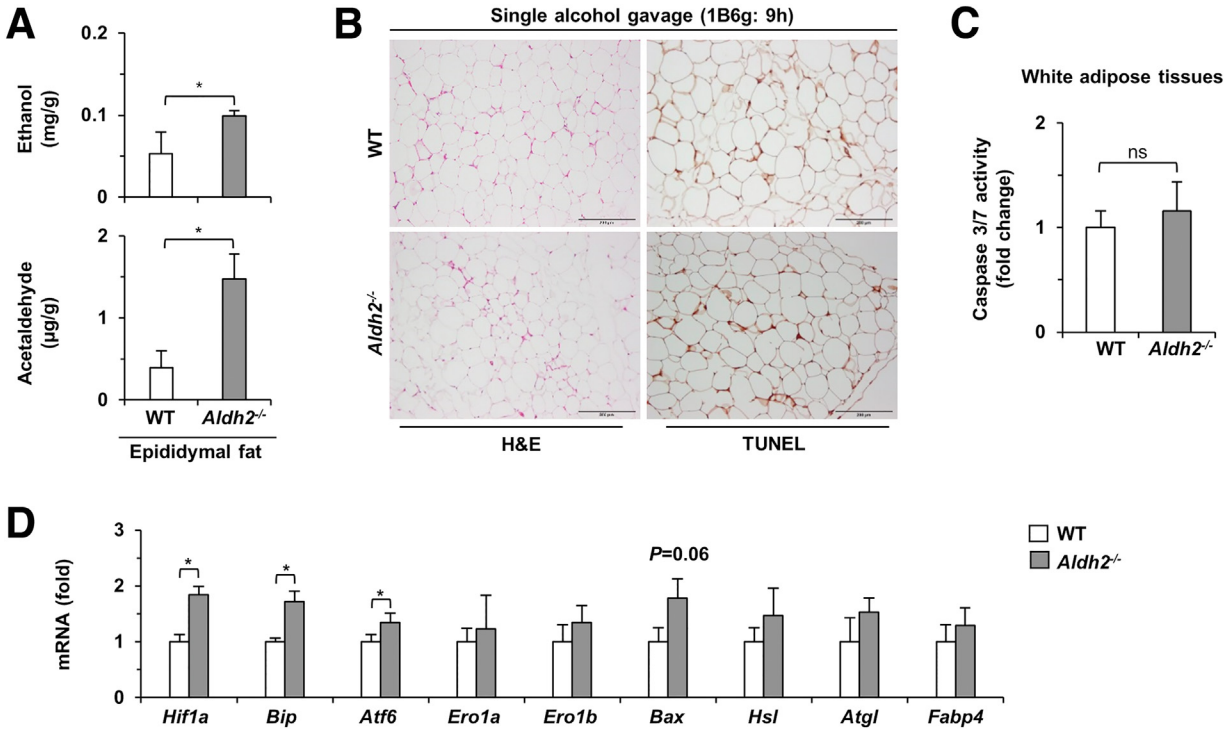

Figure 10. Ablation of the *Aldh2* gene does not affect acute alcohol-induced adipocyte death. *Aldh2*$^{-/-}$ and WT mice were subjected to a 6 g/kg single alcohol gavage and killed 9 hours after alcohol administration. (*A*) Ethanol and acetaldehyde levels in white adipose tissues were evaluated. (*B*) Representative staining images of H&E, and TUNEL staining of white adipose tissue. (*C*) Caspase 3/7 activity in epididymal fat was assessed. (*D*) White adipose tissues were subjected to RT-qPCR analysis. Data are expressed as the means ± SEM. *$P < .05$ vs the corresponding controls.

Discussion

In the current study, we extensively studied the mechanisms of ethanol binge-induced liver injury by using various lines of genetically modified mice. Several interesting findings were observed. First, ethanol, not acetaldehyde, directly contributes to acute alcohol-induced liver injury by inducing ER stress and fatty acid synthesis in the liver. Second, ethanol induces adipocyte death and lipolysis, resulting in an increase in FFAs and liver injury. Third, FAEEs, nonoxidative ethanol metabolites, contribute to acute liver injury in our ethanol binge model. Our working model of acute alcoholic liver injury is shown in the graphical abstract.

In human beings, the development of ALD is associated with the quantity and duration of alcohol consumed.[2,3] Liver is the major organ that metabolizes more than 90% of ingested alcohol into acetaldehyde through several enzymatic mechanisms,[9] although our recent studies have suggested that liver ALDH2 is responsible for less than 50% of blood acetaldehyde clearance.[11] Several studies have shown that acetaldehyde is one of the principal culprits mediating chronic alcoholic liver injury and fibrogenic effects.[10] An increased level of acetaldehyde during chronic alcohol consumption impairs cellular function by forming adducts with DNA and proteins.[10] However, the role of acetaldehyde in mediating liver injury induced by binge ethanol is not known. Binge drinking leads to a transient increase and a rapid decrease in the levels of acetaldehyde because of its very short half-life, approximately 18–31 minutes.[32] To explore the role of ethanol and acetaldehyde in acute alcoholic liver injury, we used *Adh1*$^{-/-}$ and *Aldh2*$^{-/-}$ mouse models in which ethanol metabolism was markedly inhibited. Interestingly, we found that acute alcoholic liver injury was markedly exacerbated in mice lacking the key ethanol metabolism enzyme ADH1, as indicated by an increase in serum alcohol concentration, serum aminotransferase levels, hepatic ER stress, and hepatocyte apoptosis after acute ethanol gavage. These results suggest that liver injury in an ethanol binge model likely is acetaldehyde-independent. To further test this hypothesis, we conducted experiments in mice lacking *Aldh2*, an oxidative enzyme converting acetaldehyde to acetate. Despite an increase in blood acetaldehyde after ethanol binge, *Aldh2*$^{-/-}$ mice had a similar liver injury (serum ALT levels) as WT mice. Given the combination of binge drinking and the presence of metabolic syndrome as a major risk of ALD,[7,8] we also determined the implications of ethanol and acetaldehyde in liver injury using the HFD+binge model in *Adh1*$^{-/-}$ and *Aldh2*$^{-/-}$ mice. We again observed enhanced liver injury and activation of the hepatic ER stress pathway in *Adh1*$^{-/-}$ mice challenged with HFD+binge compared with WT mice, whereas the lack of *Aldh2* did not affect liver injury in this model. Taken together, our results suggest that the mechanism underlying liver injury induced by binge ethanol intake

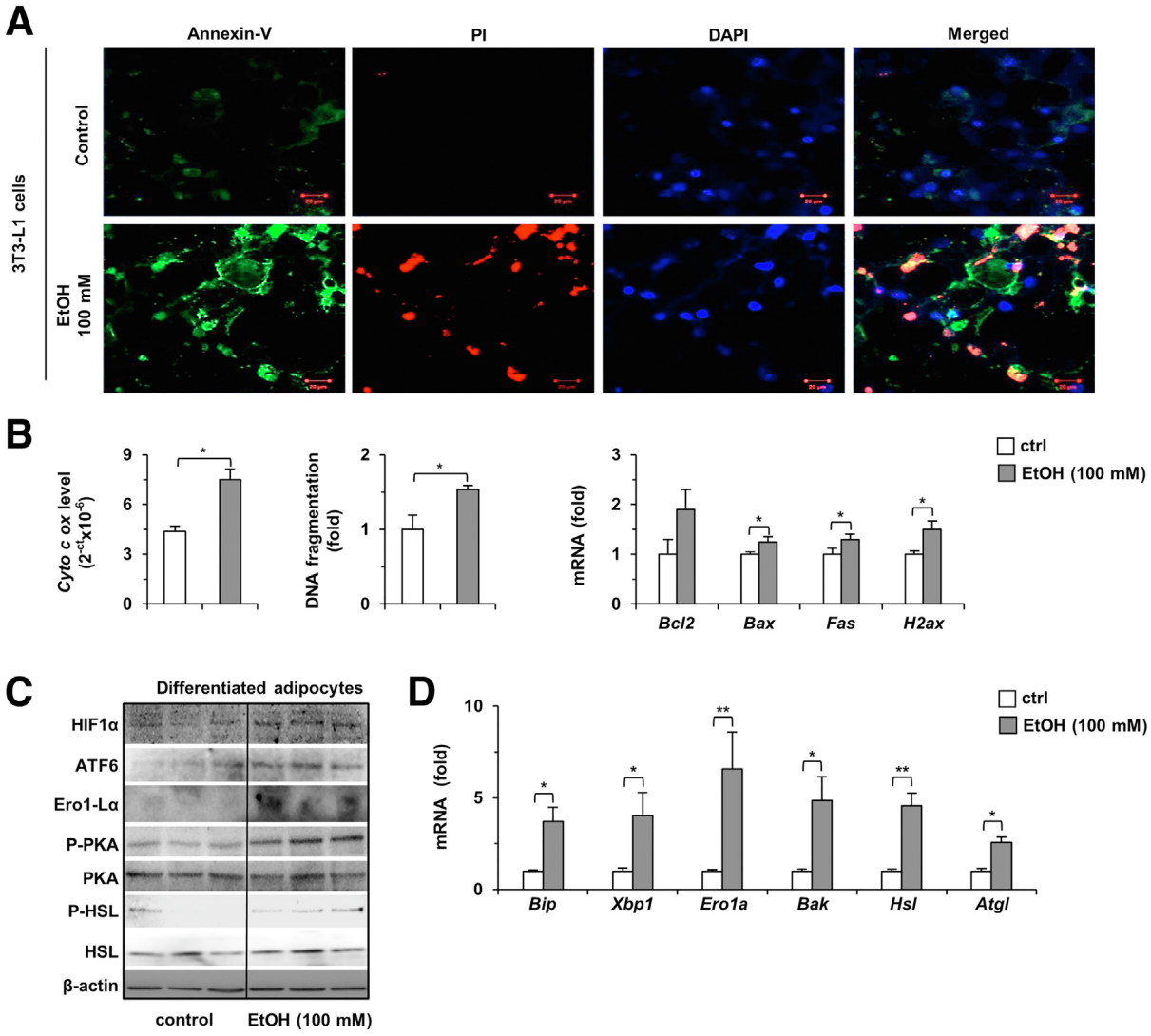

Figure 11. In vitro treatment with ethanol induces adipocyte death and ER stress. (*A* and *B*) Differentiated 3T3-L1 cells were treated with 100 mmol/L ethanol. (*A*) Representative images for annexin V and PI staining to evaluate cell death. (*B*) The copy number of mitochondrial *cyto c* ox levels from total DNA extraction and DNA fragmentation were evaluated, and the mRNA levels of cell death–associated genes were determined by RT-qPCR analysis. (*C* and *D*) Isolated stromal vascular fractions from mouse white adipose tissue were differentiated and treated with ethanol (100 mmol/L) for 24 hours. (*C*) Cultured cells were collected and analyzed using Western blot, and (*D*) mRNA expression was evaluated using RT-qPCR. Data are expressed as the means ± SEM. $^{*}P < .05$, $^{**}P < .001$ vs the corresponding controls. DAPI, 4′,6-diamidino-2-phenylindole. ctrl, control.

is acetaldehyde-independent and directly related to ethanol. This notion was confirmed further in our experiments when we found that intraperitoneal administration of ethanol, but not acetaldehyde, induces liver injury, ER stress, and hepatocyte death.

To investigate how ethanol causes liver injury in a single ethanol binge model, we carefully analyzed our transcriptomic data in the liver of mice receiving ethanol binge at 2 doses (5 and 7 g/kg). Our analyses showed that a single ethanol binge significantly up-regulated hepatic expression of genes related to fatty acid synthesis and inflammatory response but down-regulated the genes associated with fatty acid oxidation. In addition to de novo lipogenesis within the hepatocytes, adipose tissue lipolysis is another important source of hepatic fatty acids.[17,33] Alcohol disturbs adipose tissue functions by mediating adipocyte death, altering secretion of proinflammatory mediators, and release of FFAs.[34] We previously showed that adipocyte death of epididymal fat promotes liver injury by stimulating adipose tissue lipolysis, inflammation, and FFA release.[30] To conclusively address the role of adipocyte death in inducing liver injury in our ethanol binge model, we performed experiments in $Bcl2^{AdipoTg}$ mice, a model using the anti-apoptotic BCL2 protein to inhibit adipocyte death. We found that inhibition of adipocyte death ameliorated acute liver injury and hepatic ER stress in our model, suggesting

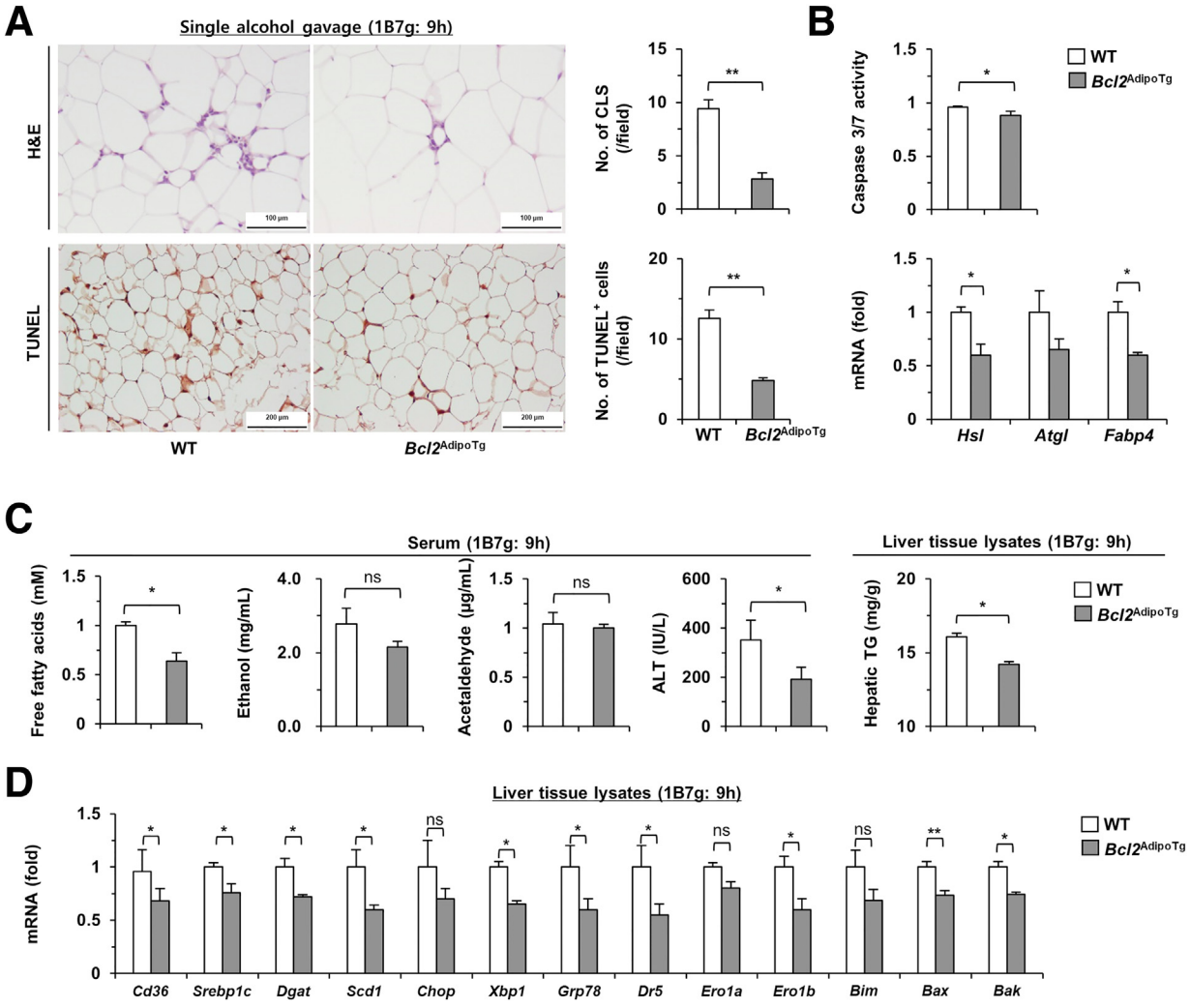

Figure 12. *Bcl2*^{AdipoTG} mice are resistant to acute ethanol-induced adipocyte death and liver injury. *Bcl2*^{AdipoTG} mice and littermate control mice were subjected to binge alcohol gavage (7 g/kg) and killed 9 hours after alcohol administration. (*A*) Representative staining images of H&E, and TUNEL staining on white adipose tissues. (*B*) Caspase 3/7 activity and RT-qPCR analysis were conducted on white adipose tissues. (*C*) Serum ethanol, acetaldehyde, FFA, and hepatic TG levels were assessed. (*D*) RT-qPCR study of liver tissue lysates. Data are expressed as the means ± SEM. **P* < .05, ***P* < .01 vs the corresponding controls.

that an increase in lipolysis secondary to adipocyte death is a driver of acute liver injury in a single ethanol binge model. Furthermore, we provided several lines of evidence suggesting that ethanol, not acetaldehyde, contributes to adipocyte death after acute ethanol gavage. First, we found a high concentration of alcohol in white adipose tissues, which was a comparable amount to that in the liver after ethanol gavage. The levels of acetaldehyde, however, were much lower in adipose tissues, likely reflecting the lower amount of ADH1 when compared with that in the liver.[35] Second, in our model, a single ethanol binge induced ER stress and adipocyte death, and activated adipose tissue lipolysis, which together likely caused an increase in circulating FFAs. These observations were augmented in *Adh1*$^{-/-}$ mice, in which we found high levels of ethanol in adipose tissues, but not in *Aldh2*$^{-/-}$ mice despite high levels of acetaldehyde in these mice. Finally, incubation with ethanol directly induced adipocyte apoptosis in vitro.

In addition to the oxidative metabolism, the liver uses a nonoxidative pathway to metabolize ethanol by combining ethanol with free fatty acids to produce lipophilic FAEEs.[12] The generation of FAEEs occurs via diverse FAEE synthase enzymes, such as FAEE carboxylesterase (encoded by *Ces1d* in murine and CES1 in human beings) and *Cel*.[13–15] The distribution of these carboxylases is tissue-specific. The *Ces1d* gene is highly expressed in the liver, while *Cel* is located primarily in the pancreas.[12,36] FAEEs are important mediators of ethanol-induced organ damage, such as alcohol-induced cardiomyopathy and alcohol-induced pancreatitis.[31,37,38] We found a significant increase in the level of circulating FAEEs, such as palmitic ethyl ester, stearic ethyl ester, and

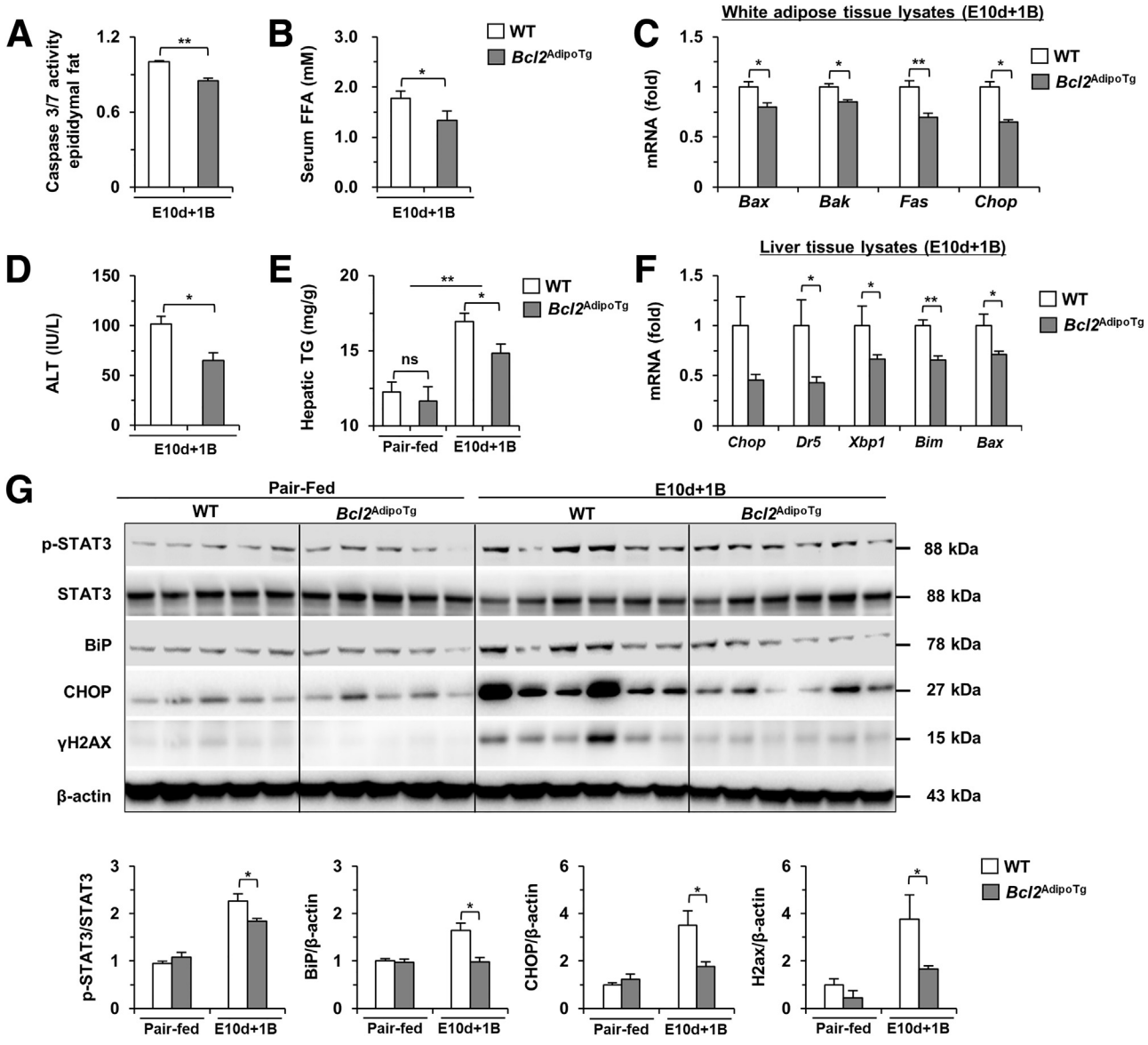

Figure 13. *Bcl2*^{AdipoTG} mice are resistant to chronic-plus-binge ethanol-induced adipocyte death, lipolysis, and hepatic ER stress. *Bcl2*^{AdipoTg} mice and their littermate control mice were subjected to E10d+1B ethanol feeding. Adipose and liver tissues were collected 9 hours postbinge. White adipose tissues were collected for the measurement of (*A*) caspase 3/7 activity, (*B*) serum FFA levels, and (*C*) RT-qPCR analyses. (*D*) Sera were collected for the measurement of ALT levels. Liver tissues were collected for the measurement of (*E*) liver TG levels, (*F*) RT-qPCR analyses of ER stress–related genes, and (*G*) Western blot analysis. Data are expressed as the means ± SEM. **P* < .05, ***P* < .01 vs the corresponding controls. STAT3, signal transducer and activator of transcription 3.

oleic ethyl ester, in mice receiving a single ethanol binge. Their levels increased further in *Adh1*$^{-/-}$ mice when ethanol oxidative metabolism is inhibited. Furthermore, deletion of *Ces1d* markedly reduced serum levels of FAEEs and hepatic ER stress, and reduced serum ALT levels after a single ethanol binge. On the other hand, deletion of *Cel*, a gene primarily expressed in the pancreas, did not affect acute liver injury after a single ethanol binge. Taken together, our results suggest an important role of hepatic FAEEs in mediating liver injury via activation of ER stress in a single ethanol binge model.

Clinical and Mechanistic Implications of This Study

Although it is believed that binge drinking exacerbates ALD, the human and animal data supporting this notion are limited.[7] An increase in the levels of serum aminotransferases has been reported among patients with alcohol intoxication, suggesting the possibility of acute liver injury in these patients.[39,40] In a large cohort of more than 6000 patients without baseline liver disease, binge drinking frequency is associated directly with ALD and its association is more pronounced in patients with metabolic syndrome.[7] The

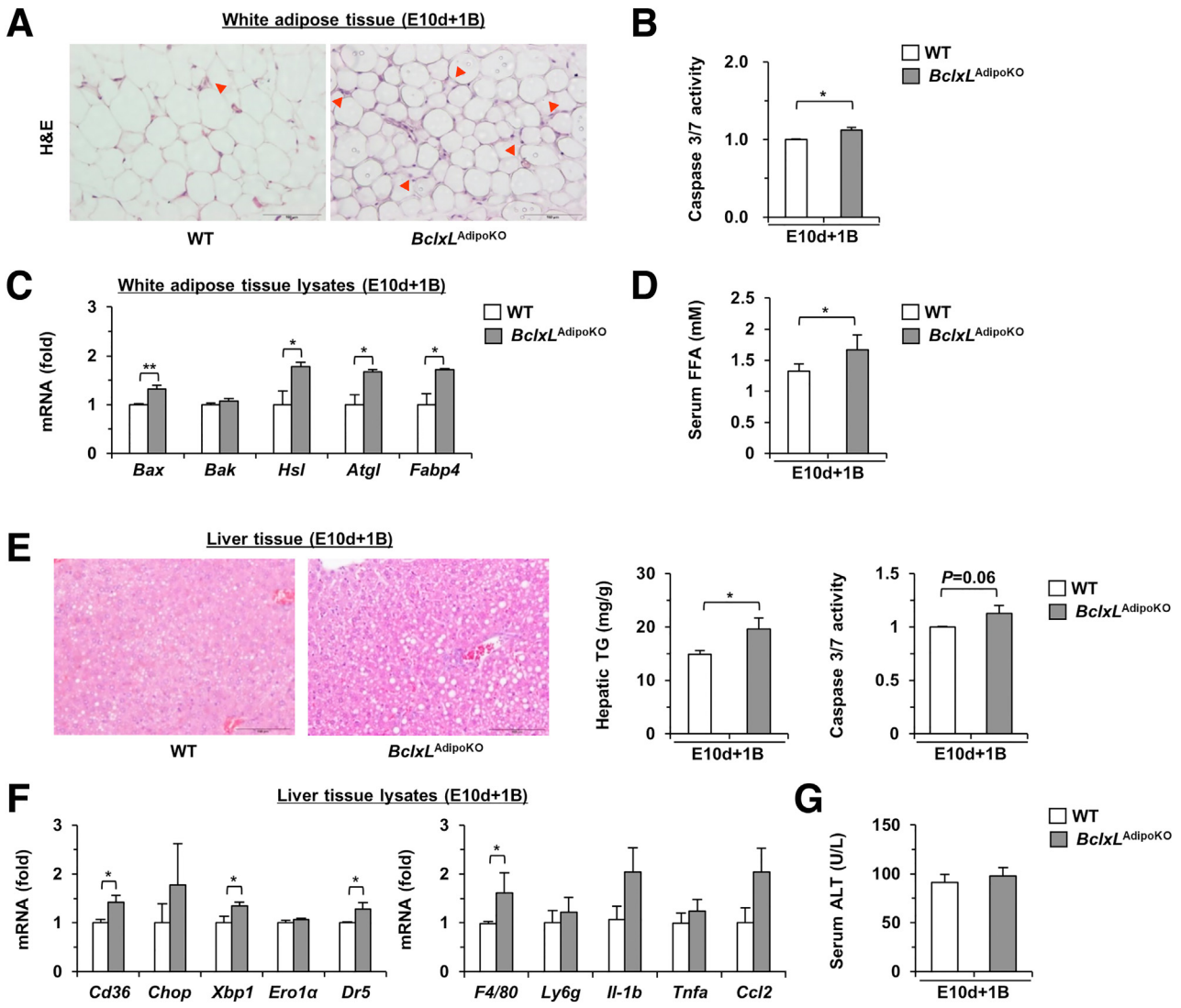

Figure 14. Deletion of the *Bcl-xL* gene in adipocytes enhances lipolysis and liver TG synthesis after chronic-plus-binge ethanol feeding. *Bcl-xL*^{AdipoKO} mice and their littermate control mice were subjected to E10d+1B ethanol feeding. Mice were killed 9 hours after the gavage for analyses. White adipose tissues were subjected to (*A*) H&E staining (crown-like structures: *arrowhead*) (*B*) the measurement of caspase 3/7 activity, and (*C*) RT-qPCR analysis. (*D*) Sera were collected for the measurement of FFA levels. Liver tissues were collected for (*E*) H&E staining, measurement of hepatic TG and caspase 3/7 activity, and (*F*) RT-qPCR analysis. (*G*) Sera were collected for the measurement of ALT levels. Data are expressed as the means ± SEM. *$P < .05$, **$P < .001$ vs the corresponding controls.

mechanism underlying these findings in human studies remains obscured. Our findings that ethanol, not acetaldehyde, is the key driver of acute liver injury in our model deserves further discussion, especially in the context of allelic variants of *ADH* and *ALDH* and their enzymatic activities to metabolize ethanol.[9] It was reported that serum ALT levels were much lower in alcohol-intoxicated patients with ALDH2*1/2 (low activity) than those with ALDH2*1/1 (full activity).[39] Whether patients with a genetic variant leading to low ADH enzymatic activity are more susceptible to acute liver injury from binge drinking should be explored further. In summary, in a single ethanol binge model, we found that ethanol and its nonoxidative metabolites (FAEEs), not acetaldehyde, promote acute alcohol-induced liver injury by inducing ER stress, adipocyte death, and lipolysis.

Materials and Methods

Animal Experiments

The following lines of genetically modified mice were used in this study: *Adh1*$^{-/-}$, *Aldh2*$^{-/-}$, *Chop*$^{-/-}$, *Cyp2e1*$^{-/-}$, *Bcl2*^{AdipoTG}, *Bcl-xL*^{AdipoKO}, and *Ces1d*$^{-/-}$ mice. In detail, *Adh1*$^{-/-}$ and *Aldh2*$^{-/-}$ mice and their WT controls were described previously.[41,42] *Chop*$^{-/-}$ mice were purchased from Jackson Laboratory (Bar Harbor, ME). *Cyp2e1*$^{-/-}$ mice were kindly provided by Dr B. J. Song (National Institute on Alcohol Abuse and Alcoholism) and backcrossed to a C57B/6N background for more than 10 generations. Cre-inducible *Bcl2* transgenic mice were described previously[43] and were used to generate adipocyte-specific *Bcl2* transgenic mice (*Bcl2*^{AdipoTG}) with *Bcl2* overexpression by crossing

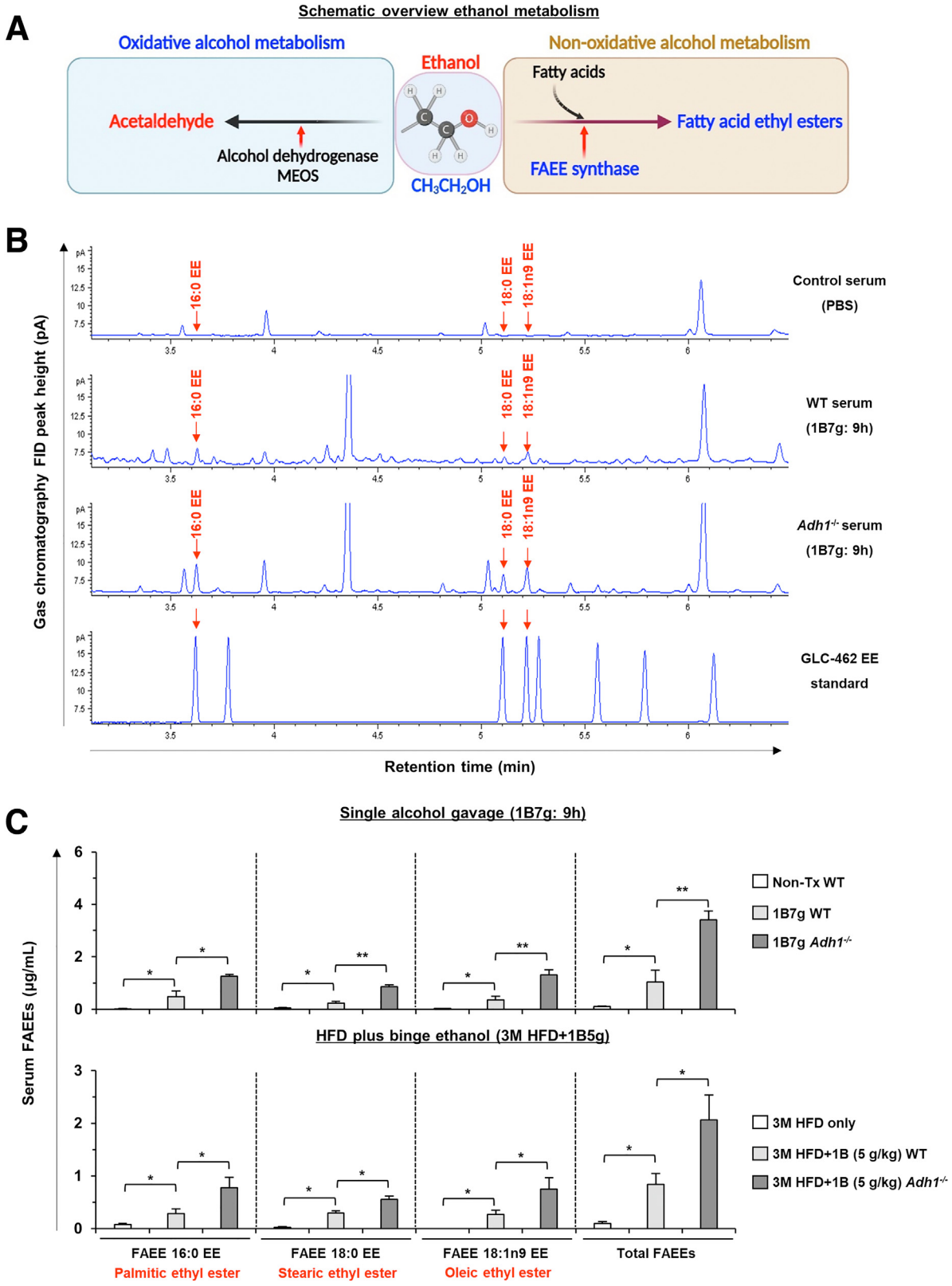

Figure 15. Binge ethanol promotes the production of FAEEs in WT and *Adh1*$^{-/-}$ mice. (*A*) A schematic overview of oxidative and nonoxidative alcohol metabolism. (*B*) Serum FAEEs were extracted using an aminopropyl column in solid-phase extraction, and FAEEs were detected using gas chromatography/flame ionization detection methods. A reference mixture of fatty acids (GLC-462, Nu-Chek Prep) was used. (*C*) Levels of serum FAEEs were evaluated using serum samples from acute alcohol binge (7 g/kg) and 3M HFD-plus-binge alcohol (5 g/kg). Data are expressed as the means ± SEM. $^{*}P < .05$, $^{**}P < .001$ vs the corresponding controls. FID, flame ionized detector; MEOS, microsomal ethanol oxidizing system; PBS, phosphate-buffered saline; 3M, 3 months.

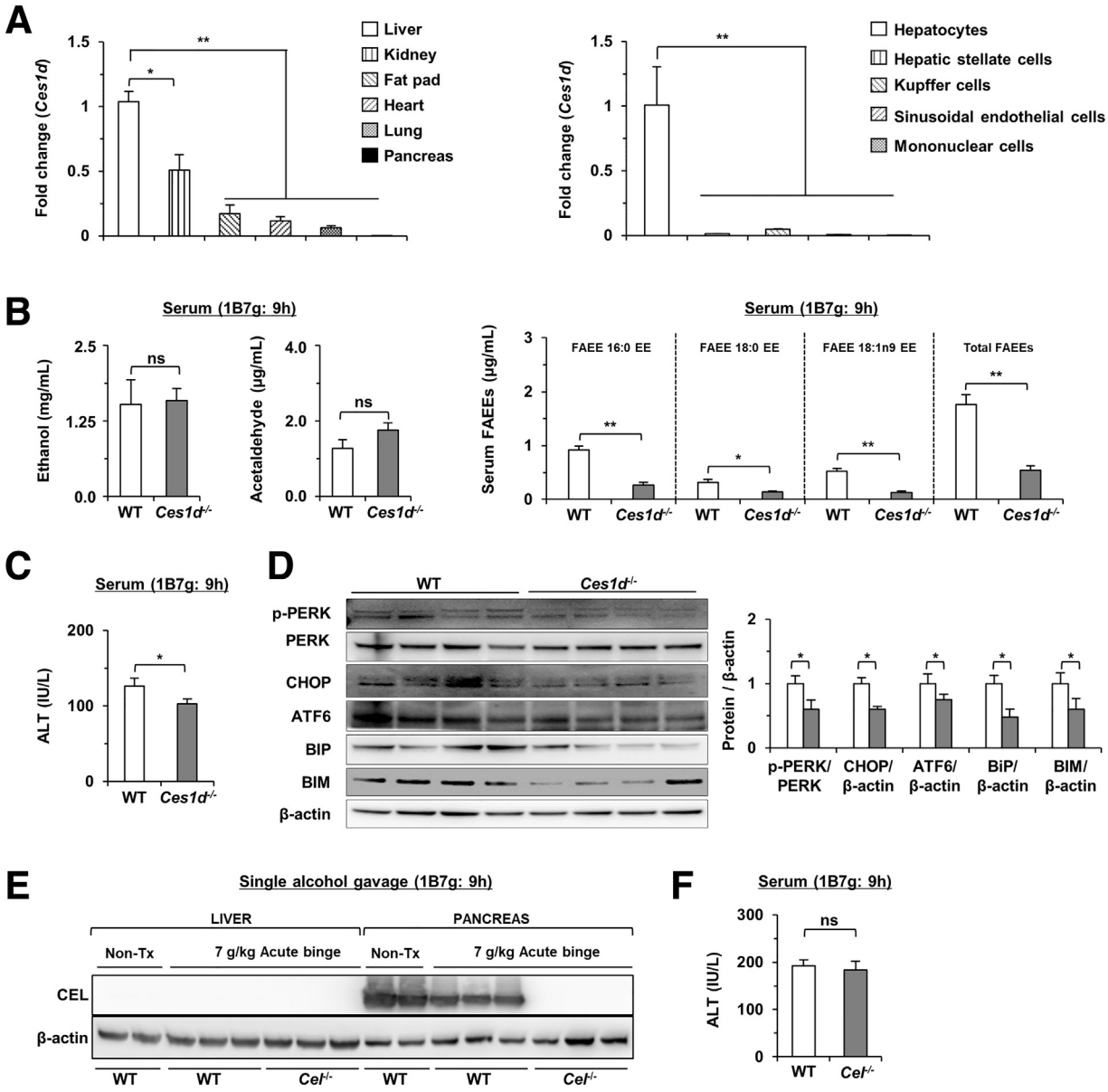

Figure 16. Deletion of the *Ces1d* gene reduces acute ethanol-induced serum FAEE and ALT increase. (*A*) RT-qPCR analysis of *Ces1d* mRNA in multiple organs and cells in the liver from C57BL/6 mice. (*B–D*) *Ces1d*$^{-/-}$ mice and littermate control mice were administered alcohol gavage (7 g/kg) and killed 9 hours after alcohol administration. (*B*) Serum ethanol, acetaldehyde, and FAEE levels were evaluated. (*C*) Serum ALT levels were evaluated. (*D*) Protein expression was assessed by Western blot on liver tissue lysates. (*E* and *F*) *Cel*$^{-/-}$ mice and littermate control mice were administered alcohol gavage (7 g/kg) and killed 9 hours after alcohol administration. (*E*) CEL protein expression in the liver and pancreas was evaluated. (*F*) Serum ALT levels were measured. Data are expressed as the means ± SEM. **P* < .05, ***P* < .001 vs the corresponding controls.

with *AdipoCre* mice (Jax Laboratory). *Bcl-xL* floxed mice were kindly provided by Dr You-Wen He (University of North Carolina) and were used to generate adipocyte-specific *Bcl-xL* KO mice by crossing with *AdipoCre* mice (Jax Laboratory). *Ces1d*$^{-/-}$ mice on a C57BL/6 background were described previously,[44] heterozygous *Ces1d*$^{+/-}$ mice were crossed to generate *Ces1d*$^{-/-}$ mice and their littermate WT controls. Unless noted, male mice were used for all experiments. Mice were housed in polycarbonate cages (maximum, 4 mice per cage) and maintained in a temperature- and light-controlled facility (12:12-hour light-dark cycle) under standard food and water ad libitum. For the induction of acute alcoholic liver injury, ethanol (5–7 g/kg) was administered orally or intraperitoneally and mice were killed at different time points. After the administration of ethanol, a heating pad (38°C) was placed under the cage to provide thermal support and to minimize body heat loss. In some experiments, mice were subjected to acute-on-chronic ethanol feeding and HFD-plus-binge ethanol feeding (denoted as 10-day chronic alcohol feeding plus single gavage and 3 months HFD+binge, respectively) using the models, as described in previous studies.[45,46] Male mice

(age, 6–7 wk) also were fed a HFD (60% kcal fat, D12492; Research Diets, New Brunswick, NJ) or a chow diet (10% kcal fat) for 3 months. In some experiments, ER stress inhibitors (PBA, cat. 8209860025, 1 mg/kg; and TUDCA, cat. 580221, 500 mg/kg; Merck-Millipore, Billerica, MA), JNK inhibitor II (cat. 420119, 20 mg/kg; Merck-Millipore), ethanol (6 g/kg), or acetaldehyde (50 mg/kg) were administered intraperitoneally. All animals received humane care in accordance with the Guide for the Care and Use of Laboratory Animals published by the National Institutes of Health. All animal experiments were approved by the National Institute on Alcohol Abuse and Alcoholism Animal Care and Use Committee.

Histologic Analysis

The liver and perigonadal adipose tissues were fixed with 10% neutral buffered formalin. After deparaffinization and rehydration, paraffin sections with 4-μm thickness were stained with H&E and Sirius Red. TUNEL staining was performed with an ApopTag Peroxidase In Situ Apoptosis Detection Kit (S7101; Merck-Millipore). Paraffin-embedded liver and adipose tissues were subjected to immunohistochemistry analyses. Endogenous peroxidases were blocked with 3% H_2O_2 for 30 minutes and nonspecific binding was blocked further with 3% normal goat serum for 1 hour. Tissues were incubated with primary antibody overnight at 4°C and incubated with the ABC staining kit (PK-4001, rabbit IgG; Vector Laboratories, Inc, Burlingame, CA). Reactions were developed with 3,3′-diaminobenzidine tetra hydrochloride peroxidase substrate (SK-4105; Vector Laboratories, Inc), according to the manufacturer's instructions, and then slides were counterstained with hematoxylin.

RT-qPCR

For RT-qPCR assays, total RNA was isolated from tissues or cells with TRIzol reagent (Thermo Fisher Scientific, Invitrogen). Total RNA was obtained and reverse-transcribed into complementary DNA (cDNA) using the High-Capacity cDNA Reverse Transcription kit (Thermo Fisher Scientific), according to the manufacturer's instructions. RT-qPCR was performed by SYBR Green Real-Time PCR master mix (Applied Biosystems). The mRNA expression levels of the target genes were normalized to β-actin mRNA expression. The mouse primer sequences are shown in Table 1 and were obtained from Thermo Fisher Scientific.

Western Blot Analysis

Tissues or cell lysates were homogenized in RIPA lysis buffer at 4°C and centrifuged at 10,000 × g for 10 minutes. After tissue homogenization, the supernatants were mixed with loading buffer and subjected to sodium dodecyl sulfate–polyacrylamide gel electrophoresis and the lysates were subjected to 4%–12% Tri-glycine gradient gels (Criterion XT; Bio-Rad). The extracted proteins were transferred onto nitrocellulose membranes. Membranes were blocked in 5% milk, incubated with primary antibodies at 1:1000 in PBS containing 0.05% Tween-20 (PBST) Protein bands were visualized by SuperSignal West Femto Maximum Sensitivity Substrate (#34096; Thermo Fisher Scientific). Comparative amounts were normalized with β-actin.

Antibodies

Primary antibodies specific for the following proteins were used. For Western blot analysis, antibodies against ADH1 (5295s; CST), ALDH2 (ab194587; Abcam), CYP2E1 (AB1252; Sigma), phosphorylated stress-activated protein kinase/Jun-amino-terminal kinase (p-SAPK/JNK) (Thr183/Tyr185) (#4668s; CST), SAPK/JNK (#9258; CST), phosphylated PERK (Thr982) (#3179s; CST), PERK (C33E10) (#3192; CST), p-eIF2α (Ser51) (#3398; CST), eIF2α (#5324; CST), p-IRE1α (phospho-S724) (ab48187; Abcam), IRE1α (14C10) (#3294; CST), X-box binding protein 1 (E9V3E) (#40435; CST), CHOP (#5554s; CST), BAD (D24A9) (#9239; CST), BIM (C34C5) (#2933; CST), BiP (#3177s; CST), p-histone H2A histone family member X (Ser139) (#9718; CST), hypoxia-inducible factor 1 alpha (D2U3T) (#14179; CST), Activating transcription factor 6 (D4Z8V) (#65880; CST), FASN (#3189; CST), SCD1 (C12H5) (#2794; CST), adipose triglyceride lipase (#2138; CST), ER oxidoreductin 1-L alpha (#3264; CST), phosphorylated protein kinase A c (Thr197) (#4781; CST), PKA c (#4782; CST), p-HSL (Ser660) (#4126; CST), HSL (#4107; CST), phosphorylated signal transducer and activator of transcription 3 (Tyr705) (#9145; CST), and STAT3 (#30835; CST) were used. Prediluted rabbit anti-F4/80 (CST) antibody was used for immunohistochemistry. Secondary antibodies for Western blot analyses were horseradish-peroxidase–linked anti-rabbit IgG (#7074; CST) and horseradish-peroxidase–linked anti-mouse IgG (#7076; CST) at 1:5000 dilutions.

Serum Biochemical Analyses

Serum was collected for the evaluation of ALT and AST using the VetTest Chemistry analyzer (IDEXX Laboratories), according to the manufacturer's instructions. Levels of serum ethanol, acetaldehyde, and hepatic FFAs were evaluated using gas chromatography–mass spectrometry. Serum FFA levels were measured with a commercial kit from BioVision (#K612; Milpitas, CA), according to the manufacturer's instructions. The results were obtained using the Infinite M200 Promicroplate reader (Tecan Group Ltd), equipped at Ewha Drug Development Research Core Center.

FAEE Identification and Quantification

A quantitative internal standard of ethyl heptadecanoate (E17:0) was added to the collected serum samples, and the lipids were extracted with acetone/hexane. Then, the FAEEs were isolated by solid-phase extraction using an aminopropyl column (1 mL/100 mg; Thermo Fisher Scientific), as described previously.[12,31,47] The purified FAEEs were separated, identified, and quantitated by gas chromatography/flame ionization detector.

Table 1. List of Primers

Name	Sequence, 5'→3'
Acta2 (for)	CTGACAGAGGCACCACTGAA
Acta2 (rev)	GAAGGAATAGCCACGCTCAG
Adh1 (for)	GCAAAGCTGCGGTGCTATG
Adh1 (rev)	TCACACAAGTCACCCCTTCTC
Aldh2 (for)	GACGCCGTCAGCAGGAAAA
Aldh2 (rev)	CGCCAATCGGTACAACAGC
Atf6 (for)	TCGCCTTTTAGTCCGGTTCTT
Atf6 (rev)	GGCTCCATAGGTCTGACTCC
Atgl (for)	CCACTCACATCTACGGAGCC
Atgl (rev)	TAATGTTGGCACCTGCTTCA
Bak (for)	AGACCTCCTCTGTGTCCTGG
Bak (rev)	AAAATGGCATCTGGACAAGG
Bax (for)	GATCAGCTCGGGCACTTTAG
Bax (rev)	TTGCTGATGGCAACTTCAAC
Bcl-xl (for)	GCTGCATTGTTCCCGTAGAG
Bcl-xl (rev)	GTTGGATGGCCACCTATCTG
Bcl2 (for)	GGTCTTCAGAGACAGCCAGG
Bcl2 (rev)	GATCCAGGATAACGGAGGCT
Bim (for)	GCCCCTACCTCCCTACAGAC
Bim (rev)	GCTCCTGTGCAATCCGTATC
Bip (for)	ATCTTTGGTTGCTTGTCGCT
Bip (rev)	ATGAAGGAGACTGCTGAGGC
Cd36 (for)	CCTGCAAATGTCAGAGGAAA
Cd36 (rev)	GCGACATGATTAATGGCACA
Chop (for)	GACCAGGTTCTGCTTTCAGG
Chop (rev)	CAGCGACAGAGCCAGAATAA
Col1a1 (for)	TAGGCCATTGTGTATGCAGC
Col1a1 (rev)	ACATGTTCAGCTTTGTGGACC
Col1a2 (for)	GGTGAGCCTGGTCAAACGG
Col1a2 (rev)	ACTGTGTCCTTTCACGCCTTT
*Col3a*1 (for)	TAGGACTGACCAAGGTGGCT
Col3a1 (rev)	GGAACCTGGTTTCTTCTCACC
Col4a1 (for)	CACATTTTCCACAGCCAGAG
Col4a1 (rev)	GTCTGGCTTCTGCTGCTCTT
Col5a2 (for)	TTGGAAACCTTCTCCATGTCAGA
Col5a2 (rev)	TCCCCAGTGGGTGTTATAGGA
Cxcl1 (for)	TCTCCGTTACTTGGGGACAC
Cxcl1 (rev)	CCACACTCAAGAATGGTCGC
Cyto C ox (for)	ACCAAGGCCACCACACTCCT
Cyto C ox (rev)	ACGCTCAGAAGAATCCTGCAAAGAA
Dgat1 (for)	GACGGCTACTGGGATCTGA
Dgat1 (rev)	TCACCACACACCAATTCAGG
Dr5 (for)	GGTCCTCTTGATGGGCTCTC
Dr5 (rev)	GTTGCTGCTTGCTGTGCTAC
Ero1a (for)	CACAGGTACAGTCGTCCAGGT
Ero1a (rev)	CTTGCTCGTTGGACTCCTG
Ero1b (for)	TGACAAAAAGGGGGCCAAGT
Ero1b (rev)	TATCGCACCCAACACAGTCC
Fabp4 (for)	AAGGTGAAGAGCATCATAACCCT
Fabp4 (rev)	TCACGCCTTTCATAACACATTCC
Fas (for)	GCGGGTTCGTGAAACTGATAA

Table 1. Continued

Name	Sequence, 5'→3'
Fas (rev)	GCAAAATGGGCCTCCTTGATA
Gadd34 (for)	GGAGATAGAAGTTGTGGGCG
Gadd34 (rev)	TTTTGGCAACCAGAACCG
Hif1a (for)	ACCTTCATCGGAAACTCCAAAG
Hif1a (rev)	CTGTTAGGCTGGGAAAAGTTAGG
Hsl (for)	CCTGCAAGAGTATGTCACGC
Hsl (rev)	GGAGAGAGTCTGCAGGAACG
H2afx (for)	GGCCTGTGGACAAGAGTTCTAT
H2afx (rev)	GCCCATTAAATCTCCCCACT
Lcn2 (for)	TGGCCCTGAGTGTCATGTG
Lcn2 (rev)	CTCTTGTAGCTCATAGATGGTGC
Ly6g (for)	TGCGTTGCTCTGGAGATAGA
Ly6g (rev)	CAGAGTAGTGGGGCAGATGG
Pdi (for)	CCCCGTGTGTGGAAAAGAGA
Pdi (rev)	AGCCACAGAGTAATGTGCCC
Srebp1 (for)	GGAGCCATGGATTGCACATT
Srebp1 (rev)	GGCCCGGGAAGTCACTGT
Trail (for)	GGTCCTCTTGATGGGCTCTC
Trail (rev)	GTTGCTGCTTGCTGTGCTAC
Xbp1 (for)	AGCAGCAAGTGGTGGATTTG
Xbp1 (rev)	GAGTTTTCTCCCGTAAAAGCTGA
18S (for)	AACTTTCGATGGTAGTCGCCGT
18S (rev)	TCCTTGGATGTGGTAGCCGTTT
Actb (for)	GGCTGTATTCCCCTCCATCG
Actb (rev)	CCAGTTGGTAACAATGCCATGT

for, forward; rev, reverse.

GTT and ITT

Animals were fasted overnight for GTT and fasted for 6 hours for ITT. Blood was collected through tail vein at 0, 15, 30, 45, 60, and 120 minutes after intraperitoneal injection of glucose (0.75 g/kg) or insulin (1.5 IU/kg). The glucose levels were measured by a digital glucometer.

Immunofluorescence Staining

The cultured cells were stained with an Annexin V/PI double staining kit (#101-100; BioVision) to detect cell death, according to the manufacturer's instructions. The images were obtained using a LSM710 confocal microscope (Zeiss, Thornwood, NY).

Cell Death Assay

DNA fragmentation was measured with a cell death detection kit (#11544675001; Roche). Samples were prepared and measured according to the manufacturer's instructions. Caspase 3/7 activities in the adipose tissue samples were measured with a commercial kit (#G7791; Promega, Madison, WI), according to the manufacturer's instructions.

Isolation of Stromal Vascular Fraction Cells

Perigonadal adipose tissues were harvested from mice and digested with collagenase A (#10103578001; Roche). Adipocytes and preadipocytes were separated by centrifugation (1500 rpm, 5 min), and preadipocytes were resuspended for adipocyte differentiation.

Cell Culture

Cells were cultured in Dulbecco's modified Eagle medium supplemented with 10% fetal bovine serum and penicillin/streptomycin solution (#15140122; Gibco) and maintained in a humidified incubator at 37°C and 5% CO_2. After reaching confluence, 3T3-L1 or stromal vascular fraction cells were cultured with 10% fetal bovine serum, 0.125 mmol/L indomethacin, 1 μmol/L dexamethasone, 0.5 mmol/L IBMX, 0.02 μmol/L insulin, and 1 μmol/L rosiglitazone to induce differentiation for 2 days. The media then were replaced with 10% fetal bovine serum, insulin, and rosiglitazone. The media were renewed every 2–3 days during cell culture.

Microarray Analyses of Mouse Liver Samples

Liver samples from mice with ethanol (5 or 7 g/kg) gavage or maltose (control) were subjected to microarray analysis. Dye-coupled cDNAs were isolated by using a MiniElute PCR purification kit (Qiagen) and hybridized to an Agilent 44K mouse 60-mer oligo microarray (Agilent Technologies, Santa Clara, CA). The Genespring GX software package (Agilent Technologies) was used to process and normalize the data. The raw data from the maltose control and 5-g/kg ethanol groups were published previously and deposited in NCBI's Gene Expression Omnibus (accession number: GSE98153).[48] The liver tissue microarray data from 7-g/kg ethanol gavaged mice have been deposited in NCBI's Gene Expression Omnibus (GSE214778). Differential expression analysis was performed via the R package DESeq2 (v1.30.1). Genes with fold change >1.5 and an adjusted P value less than .05 were put into gene set enrichment analysis via the R package cluster Profiler (v3.18.1). The R package heatmap (v1.0.12) was used to generate the heatmap plots. Interactive Venn diagrams and gene function analyses were processed by ingenuity pathway analysis.

Statistical Analysis

Data are presented as means ± SEM (n = 6–15 per group). Statistical analysis was performed using the 2-tailed Student t test or 1-way analysis of variance. All $P < .05$ values were considered statistically significant.

References

1. Liangpunsakul S, Haber P, McCaughan GW. Alcoholic liver disease in Asia, Europe, and North America. Gastroenterology 2016;150:1786–1797.
2. Teli MR, Day CP, Burt AD, Bennett MK, James OF. Determinants of progression to cirrhosis or fibrosis in pure alcoholic fatty liver. Lancet 1995;346:987–990.
3. Becker U, Deis A, Sorensen TI, Gronbaek M, Borch-Johnsen K, Muller CF, Schnohr P, Jensen G. Prediction of risk of liver disease by alcohol intake, sex, and age: a prospective population study. Hepatology 1996;23:1025–1029.
4. Fillmore MT, Jude R. Defining "binge" drinking as five drinks per occasion or drinking to a .08% BAC: which is more sensitive to risk? Am J Addict 2011;20:468–475.
5. Tapper EB, Parikh ND. Mortality due to cirrhosis and liver cancer in the United States, 1999-2016: observational study. BMJ 2018;362:k2817.
6. Wong T, Dang K, Ladhani S, Singal AK, Wong RJ. Prevalence of alcoholic fatty liver disease among adults in the United States, 2001-2016. JAMA 2019;321:1723–1725.
7. Ventura-Cots M, Watts AE, Bataller R. Binge drinking as a risk factor for advanced alcoholic liver disease. Liver Int 2017;37:1281–1283.
8. Aberg F, Helenius-Hietala J, Puukka P, Jula A. Binge drinking and the risk of liver events: a population-based cohort study. Liver Int 2017;37:1373–1381.
9. Jiang Y, Zhang T, Kusumanchi P, Han S, Yang Z, Liangpunsakul S. Alcohol metabolizing enzymes, microsomal ethanol oxidizing system, cytochrome P450 2E1, catalase, and aldehyde dehydrogenase in alcohol-associated liver disease. Biomedicines 2020;8:50.
10. Setshedi M, Wands JR, Monte SM. Acetaldehyde adducts in alcoholic liver disease. Oxid Med Cell Longev 2010;3:178–185.
11. Guillot A, Ren T, Jourdan T, Pawlosky RJ, Han E, Kim SJ, Zhang L, Koob GF, Gao B. Targeting liver aldehyde dehydrogenase-2 prevents heavy but not moderate alcohol drinking. Proc Natl Acad Sci U S A 2019;116:25974–25981.
12. Huang W, Booth DM, Cane MC, Chvanov M, Javed MA, Elliott VL, Armstrong JA, Dingsdale H, Cash N, Li Y, Greenhalf W, Mukherjee R, Kaphalia BS, Jaffar M, Petersen OH, Tepikin AV, Sutton R, Criddle DN. Fatty acid ethyl ester synthase inhibition ameliorates ethanol-induced Ca2+-dependent mitochondrial dysfunction and acute pancreatitis. Gut 2014;63:1313–1324.
13. Lange LG. Nonoxidative ethanol metabolism: formation of fatty acid ethyl esters by cholesterol esterase. Proc Natl Acad Sci U S A 1982;79:3954–3957.
14. Tsujita T, Okuda H. Fatty acid ethyl ester synthase in rat adipose tissue and its relationship to carboxylesterase. J Biol Chem 1992;267:23489–23494.
15. Holmes RS, Wright MW, Laulederkind SJ, Cox LA, Hosokawa M, Imai T, Ishibashi S, Lehner R, Miyazaki M, Perkins EJ, Potter PM, Redinbo MR, Robert J, Satoh T, Yamashita T, Yan B, Yokoi T, Zechner R, Maltais LJ. Recommended nomenclature for five mammalian carboxylesterase gene families: human, mouse, and rat genes and proteins. Mamm Genome 2010;21:427–441.
16. Gao B, Ahmad MF, Nagy LE, Tsukamoto H. Inflammatory pathways in alcoholic steatohepatitis. J Hepatol 2019;70:249–259.
17. Liangpunsakul S, Chalasani N. Lipid mediators of liver injury in nonalcoholic fatty liver disease. Am J Physiol Gastrointest Liver Physiol 2019;316:G75–G81.

18. Sebastian BM, Roychowdhury S, Tang H, Hillian AD, Feldstein AE, Stahl GL, Takahashi K, Nagy LE. Identification of a cytochrome P4502E1/Bid/C1q-dependent axis mediating inflammation in adipose tissue after chronic ethanol feeding to mice. J Biol Chem 2011; 286:35989–35997.
19. Zhong W, Zhao Y, Tang Y, Wei X, Shi X, Sun W, Sun X, Yin X, Sun X, Kim S, McClain CJ, Zhang X, Zhou Z. Chronic alcohol exposure stimulates adipose tissue lipolysis in mice: role of reverse triglyceride transport in the pathogenesis of alcoholic steatosis. Am J Pathol 2012;180:998–1007.
20. Mathur M, Yeh YT, Arya RK, Jiang L, Pornour M, Chen W, Ma Y, Gao B, He L, Ying Z, Xue B, Shi H, Choi Y, Yu L. Adipose lipolysis is important for ethanol to induce fatty liver in the National Institute on Alcohol Abuse and Alcoholism murine model of chronic and binge ethanol feeding. Hepatology 2022, Epub ahead of print.
21. Wei X, Shi X, Zhong W, Zhao Y, Tang Y, Sun W, Yin X, Bogdanov B, Kim S, McClain C, Zhou Z, Zhang X. Chronic alcohol exposure disturbs lipid homeostasis at the adipose tissue-liver axis in mice: analysis of triacylglycerols using high-resolution mass spectrometry in combination with in vivo metabolite deuterium labeling. PLoS One 2013;8: e55382.
22. Gao B, Xu MJ, Bertola A, Wang H, Zhou Z, Liangpunsakul S. Animal models of alcoholic liver disease: pathogenesis and clinical relevance. Gene Expr 2017;17:173–186.
23. Sanz-Garcia C, Poulsen KL, Bellos D, Wang H, McMullen MR, Li X, Chattopadhyay S, Sen G, Nagy LE. The non-transcriptional activity of IRF3 modulates hepatic immune cell populations in acute-on-chronic ethanol administration in mice. J Hepatol 2019; 70:974–984.
24. Wang L, You HM, Meng HW, Pan XY, Chen X, Bi YH, Zhang YF, Li JJ, Yin NN, Zhang ZW, Huang C, Li J. STING-mediated inflammation contributes to Gao binge ethanol feeding model. J Cell Physiol 2022; 237:1471–1485.
25. Wang S, Ni HM, Chao X, Ma X, Kolodecik T, De Lisle R, Ballabio A, Pacher P, Ding WX. Critical role of TFEB-mediated lysosomal biogenesis in alcohol-induced pancreatitis in mice and humans. Cell Mol Gastroenterol Hepatol 2020;10:59–81.
26. Ma J, Guillot A, Yang Z, et al. Distinct histopathological phenotypes of severe alcoholic hepatitis suggest different mechanisms driving liver injury and failure. J Clin Invest 2022;132(14):e157780.
27. Jeanblanc J, Rolland B, Gierski F, Martinetti MP, Naassila M. Animal models of binge drinking, current challenges to improve face validity. Neurosci Biobehav Rev 2019;106:112–121.
28. Cai Y, Xu MJ, Koritzinsky EH, Zhou Z, Wang W, Cao H, Yuen PS, Ross RA, Star RA, Liangpunsakul S, Gao B. Mitochondrial DNA-enriched microparticles promote acute-on-chronic alcoholic neutrophilia and hepatotoxicity. JCI Insight 2017;2:e92634.
29. Hu H, Tian M, Ding C, Yu S. The C/EBP homologous protein (CHOP) transcription factor functions in endoplasmic reticulum stress-induced apoptosis and microbial infection. Front Immunol 2018;9:3083.
30. Kim SJ, Feng D, Guillot A, Dai S, Liu F, Hwang S, Parker R, Seo W, He Y, Godlewski G, Jeong WI, Lin Y, Qin X, Kunos G, Gao B. Adipocyte death preferentially induces liver injury and inflammation through the activation of chemokine (C-C Motif) receptor 2-positive macrophages and lipolysis. Hepatology 2019; 69:1965–1982.
31. Best CA, Laposata M. Fatty acid ethyl esters: toxic non-oxidative metabolites of ethanol and markers of ethanol intake. Front Biosci 2003;8:e202–e217.
32. Jones AW, Neiman J, Hillbom M. Elimination kinetics of ethanol and acetaldehyde in healthy men during the calcium carbimide-alcohol flush reaction. Alcohol Alcohol Suppl 1987;1:213–217.
33. Donnelly KL, Smith CI, Schwarzenberg SJ, Jessurun J, Boldt MD, Parks EJ. Sources of fatty acids stored in liver and secreted via lipoproteins in patients with nonalcoholic fatty liver disease. J Clin Invest 2005; 115:1343–1351.
34. Parker R, Kim SJ, Gao B. Alcohol, adipose tissue and liver disease: mechanistic links and clinical considerations. Nat Rev Gastroenterol Hepatol 2018;15:50–59.
35. Crabb DW, Zeng Y, Liangpunsakul S, Jones R, Considine R. Ethanol impairs differentiation of human adipocyte stromal cells in culture. Alcohol Clin Exp Res 2011;35:1584–1592.
36. Satoh T, Hosokawa M. Carboxylesterases: structure, function and polymorphism. Biomol Ther 2009; 17:335–347.
37. Beckemeier ME, Bora PS. Fatty acid ethyl esters: potentially toxic products of myocardial ethanol metabolism. J Mol Cell Cardiol 1998;30:2487–2494.
38. Kaphalia BS, Cai P, Khan MF, Okorodudu AO, Ansari GA. Fatty acid ethyl esters: markers of alcohol abuse and alcoholism. Alcohol 2004;34:151–158.
39. Tseng YM, Jin YR, Chen IJ, Huang FD, Wu SH, Ma H, Chen SY, Tsai LY, Tsai SM, Lee JH. Roles of the genetic variation of alcohol-metabolizing enzymes on biomarkers in trauma patients with excessive alcohol intake at emergency department. Clin Chim Acta 2008;389: 14–18.
40. Ren R, He Y, Ding D, Cui A, Bao H, Ma J, Hou X, Li Y, Feng D, Li X, Liangpunsakul S, Gao B, Wang H. Aging exaggerates acute-on-chronic alcohol-induced liver injury in mice and humans by inhibiting neutrophilic sirtuin 1-C/EBPalpha-miRNA-223 axis. Hepatology 2022; 75:646–660.
41. Deltour L, Foglio MH, Duester G. Metabolic deficiencies in alcohol dehydrogenase Adh1, Adh3, and Adh4 null mutant mice. Overlapping roles of Adh1 and Adh4 in ethanol clearance and metabolism of retinol to retinoic acid. J Biol Chem 1999;274:16796–16801.
42. Kitagawa K, Kawamoto T, Kunugita N, Tsukiyama T, Okamoto K, Yoshida A, Nakayama K, Nakayama K. Aldehyde dehydrogenase (ALDH) 2 associates with oxidation of methoxyacetaldehyde; in vitro analysis with

liver subcellular fraction derived from human and Aldh2 gene targeting mouse. FEBS Lett 2000;476:306–311.
43. Xiang X, Feng D, Hwang S, Ren T, Wang X, Trojnar E, Matyas C, Mo R, Shang D, He Y, Seo W, Shah VH, Pacher P, Xie Q, Gao B. Interleukin-22 ameliorates acute-on-chronic liver failure by reprogramming impaired regeneration pathways in mice. J Hepatol 2020; 72:736–745.
44. Wei E, Ben Ali Y, Lyon J, Wang H, Nelson R, Dolinsky VW, Dyck JR, Mitchell G, Korbutt GS, Lehner R. Loss of TGH/Ces3 in mice decreases blood lipids, improves glucose tolerance, and increases energy expenditure. Cell Metab 2010;11:183–193.
45. Bertola A, Mathews S, Ki SH, Wang H, Gao B. Mouse model of chronic and binge ethanol feeding (the NIAAA model). Nat Protoc 2013;8:627–637.
46. Chang B, Xu MJ, Zhou Z, Cai Y, Li M, Wang W, Feng D, Bertola A, Wang H, Kunos G, Gao B. Short- or long-term high-fat diet feeding plus acute ethanol binge synergistically induce acute liver injury in mice: an important role for CXCL1. Hepatology 2015;62:1070–1085.
47. Kaluzny MA, Duncan LA, Merritt MV, Epps DE. Rapid separation of lipid classes in high yield and purity using bonded phase columns. J Lipid Res 1985;26:135–140.
48. Zhou Z, Xu MJ, Cai Y, Wang W, Jiang JX, Varga ZV, Feng D, Pacher P, Kunos G, Torok NJ, Gao B. Neutrophil-hepatic stellate cell interactions promote fibrosis in experimental steatohepatitis. Cell Mol Gastroenterol Hepatol 2018;5:399–413.

Received May 15, 2022. Accepted October 5, 2022.

Correspondence
Address correspondence to: Bin Gao, MD, PhD, Laboratory of Liver Diseases, National Institute on Alcohol Abuse and Alcoholism, National Institutes of Health, 5625 Fishers Lane, Bethesda, Maryland 20892. e-mail: bgao@mail.nih.gov.

CRediT Authorship Contributions
Seol Hee Park (Conceptualization: Lead; Data curation: Lead; Formal analysis: Lead; Writing – original draft: Lead)
Wonhyo Seo (Conceptualization: Lead; Data curation: Lead; Formal analysis: Lead; Writing – original draft: Lead)
Mingjiang Xu (Conceptualization: Equal; Methodology: Equal)
Byran Mackowiak (Methodology: Supporting)
Yuhong Lin (Methodology: Supporting)
Yong He (Methodology: Supporting)
Yaojie Fu (Methodology: Supporting)
Seonghwang Hwang (Methodology: Supporting)
Seung-Jin Kim (Methodology: Supporting)
Yukun Guan (Methodology: Supporting)
Dechun Feng (Methodology: Supporting)
liqing Yu (Methodology: Supporting)
Richard Lehner (Methodology: Supporting)
Suthat Liangpunsakul (Methodology: Supporting)
Bin Gao, MD, PhD (Conceptualization: Lead; Data curation: Supporting; Formal analysis: Supporting; Funding acquisition: Lead; Supervision: Lead; Writing – review & editing: Lead)

Conflicts of interest
The authors disclose no conflicts.

Funding
This work was supported by the intramural program of the National Institute on Alcohol Abuse and Alcoholism, National Institutes of Health (B.G.). Seol Hee Park and Wonhyo Seo were supported in part by the National Research Foundation of Korea fellowships (2018R1A5A2025286 and 2022R1C1C1008912) when they were at the National Institute on Alcohol Abuse and Alcoholism.